endogenous transcriptional regulation.[17–21] Recently, several skin diseases have been reported to improve after decoy ODN therapy.[22,23] We, therefore, hypothesized that the acute and chronic CHS response in contact dermatitis or eczema might also improve by the transfection of STAT6 decoy ODN. If the expression of Th2 cytokine is involved in the development of CHS, then the most important step in the process of CHS might be suppressed by STAT6 decoy ODN *in vivo*. These studies demonstrated that the transfection of STAT6 decoy ODN during the induction phase of CHS resulted in a significant improvement of CHS. Since the role of STAT6 is limited in IL-4 signaling, the side effects by STAT6 decoy ODN would thus be expected to be slight. There are few therapies for severe eczema, contact dermatitis and atopic dermatitis except for systemic glucocorticoids or immunesuppresants, which have several side effects. The application of STAT6 decoy ODN appears to provide a novel therapeutic effect without any significant local or adverse effects.

Results

Diminished CHS response to TNCB in STAT6 $^{-/-}$ mice

Our initial experiments were conducted to determine whether or not the repeated epicutaneous application of TNCB could result in a shift to an earlier point in the time course of the CHS response as had been demonstrated in previous reports[13] (Figure 1a,b). As shown in Figure 1a and b, repeated TNCB application induced a shift in the pattern of the CHS response. To further evaluate the capacity of STAT6$^{-/-}$ mice to develop a CHS reaction, we compared the ear-swelling response of STAT6$^{-/-}$ mice with WT (C57BL/6) mice in acute and chronic TNCB-induced CHS. The peak response of ear swelling was detected at 4 and 24 h after the challenge in acute CHS to TNCB in WT mice, whereas, a peak response was observed at 24 h after challenge in STAT6$^{-/-}$ mice (Figure 1a). On the other hand, the peak response in ear swelling was detected only at 6 h after challenge in chronic CHS to TNCB in both WT mice and STAT6$^{-/-}$ mice (Figure 1b). As shown in Figure 1a, b, in comparison with STAT6$^{-/-}$ mice, 61% suppression of ear swelling was observed in acute CHS (a) and 59% suppression was observed in chronic CHS (b).

Histopathology of TNCB-induced CHS response in WT and STAT6$^{-/-}$ mice

We performed a histological analysis of the challenged skin in STAT6$^{-/-}$ mice and WT mice. As shown in Figure 1c, strong edema was observed in the challenged skin of WT mice demonstrating an acute and chronic CHS response, however, edematous change was weak in the STAT6$^{-/-}$ mice. An inflammatory response with a strong infiltration of eosinophils and mononuclear cells was observed in WT mice after challenge in acute and chronic CHS. In contrast, only a mild inflammatory response with a diminished infiltration of mononuclear cells and eosinophils was observed in the challenged skin of both acute and chronic CHS in STAT6$^{-/-}$ mice (Figure 1c).

In vivo transfection of fluorescence isothiocyanate-labeled ODN into the skin

In order to evaluate the efficacy and localization of the delivered STAT6 decoy ODN with HVJ-E, we introduced fluorescence isothionated-labeled decoy ODN against STAT6 with HVJ-E into the mouse skin by means of a subcutaneous injection with HVJ-E. It is noteworthy that FITC-labeled STAT6 decoy ODN was more strongly expressed in the cytoplasm of dermal cells than the control skins transfected into an empty envelope (Figure 2a, b).

In vivo transfection of STAT6 decoy ODN

To confirm that STAT6 decoy ODN with HVJ-E inhibits the binding of STAT6, nuclear extracts from ear tissues injected with STAT6 decoy ODN were obtained, and a gel-shift analysis was performed with a radiolabeled STAT5/6 probe. Figure 2c showed that the challenge with TNCB resulted in the activation of STAT6 (line 2). The increased STAT6 binding was abolished by excess amounts of cold STAT6 probe (line 5). Furthermore, the *in vivo* transfection of STAT6 decoy ODN with HVJ-E, but not scrambled decoy ODN with HVJ-E (line 4) markedly inhibited the increased STAT6 binding (line 3). These data indicate the interference of STAT6 activation by *in vivo* transfection of STAT6 decoy ODN.

Inhibition of both the acute and chronic CHS to TNCB, DNFB, and Oxa by the transfection of STAT6 decoy ODN

To determine the inhibition of decoy ODN against STAT6 in terms of the response of CHS, the ear-swelling response challenged with TNCB was examined with or without the administration of STAT6 decoy ODN or scrambled decoy ODN. STAT6 decoy ODN inhibited both the acute (Figure 3a) and chronic (Figure 3b) CHS responses significantly. % Inhibition of acute CHS or chronic CHS was 62 or 63%, respectively. To optimize the effective dose of STAT6 decoy ODN, the ear-swelling responses were examined by the injection of several doses of STAT6 decoy ODN with 0.2, 2, and 20 μM. As shown in Figure 3c, 20 μM, but not 0.2 μM, 2 μM of STAT6 decoy ODN effectively inhibited the CHS response.

To examine whether or not similar effects were observed in CHS to other haptens, we induced CHS to DNFB (Figure 3d, e), Oxa (Figure 3f, g). STAT6 decoy ODN significantly inhibited both the acute CHS to DNFB (Figure 3d) and chronic (Figure 3e, g) CHS response to DNFB, 67 or 62%, respectively. STAT6 decoy ODN also inhibited both acute CHS to Oxa (Figure 3f) and chronic CHS to Oxa (Figure 3 g).

Histopathology of the acute and chronic CHS response in mice treated with or without STAT6 decoy ODN

We performed a histopathological analysis of TNCB-induced skin injected with or without STAT6 decoy ODN or scrambled decoy. As shown in Figure 4a, marked dermal edema was detected in the challenged skin of either nontransfected (positive control) or scrambled decoy ODN-transfected mice in both acute and chronic CHS to TNCB, however, edematous change was weak in the mice transfected with STAT6 decoy ODN. An inflammatory response with a strong cellular infiltration was observed in nontransfected or scrambled decoy

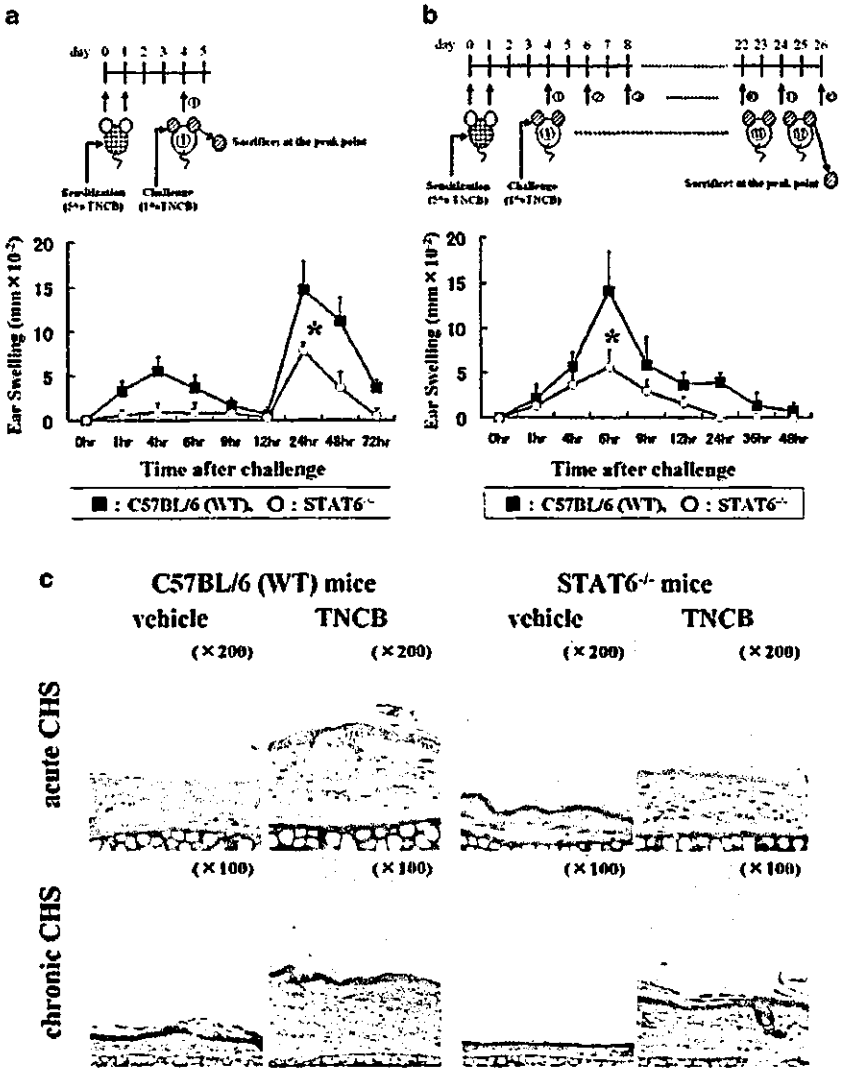

*Figure 1 STAT6-deficient (STAT6$^{-/-}$) mice exhibit both reduced acute and chronic CHS responses. (a) Acute CHS: C57BL/6 STAT6$^{-/-}$ mice (○: TNCB-STAT6$^{-/-}$) and C57BL/6 (WT) mice (■: TNCB-WT) were sensitized with 5% TNCB solution on shaved abdominal skin and challenged with 1% TNCB solution on day 4. The maximal ear swelling was detected at 24 h after the first application. (b) Chronic CHS: C57BL/6 STAT6$^{-/-}$ mice (○: TNCB-STAT6$^{-/-}$) and C57BL/6 (WT) mice (■: TNCB-WT) were sensitized with 5% TNCB solution on shaved abdominal skin and challenged 12 times with 1% TNCB solution every other day on ear lobes from day 4 to 26. The maximal ear swelling was detected at 6 h after 12th application. The data presented are the mean values ± s.d. of at least five mice per group. *$P<0.01$, significant compared with the results of WT mice. (c) Histopathological findings of the acute/chronic CHS induced in WT or STAT6$^{-/-}$ mice stained with Giemsa solution. At the last challenge, each ear lobe was challenged with vehicle or TNCB. An extremely large degree of edema was detected in the TNCB-challenged skin in the WT mice, but edematous change was weak in the STAT6$^{-/-}$ mice in both acute and chronic CHS. A strong inflammatory cellular infiltration was observed in the dermis of the positive control WT mice in acute and chronic CHS.*

ODN-transfected mice at 24 h after challenge in acute CHS and also at 4 h after challenge in chronic CHS (Figure 4a). In contrast, only a mild inflammatory response with a diminished infiltration was observed in the challenged skin in STAT6 decoy ODN-transfected mice in acute CHS. However, a remarkable cellular infiltration was still observed in the STAT6 decoy ODN-transfected mice in chronic CHS (Figure 4a). The number of infiltrated mononuclear cells, eosinophils, neutrophils, mast cells and degranulated mast cells in the skin was calculated in the scrambled or STAT6 decoy ODN-transfected mice and nontransfected mice in both acute and chronic CHS (Figure 4b–e). TNCB-challenged mice (positive control) and the mice transfected with scrambled decoy ODN had a greater number of mononuclear cells, eosinophils, mast cells and especially degranulated mast cells. The number of mononuclear cells in acute (b) and chronic (c) CHS showed a 30% suppression in mice by the transfection of STAT6 decoy ODN (Figure 4b, c). An 93% suppression of eosinophils infiltration in acute CHS and a 67% suppression of that in chronic CHS were observed in mice transfected with STAT6 Decoy ODN (Figure 4d, e). However, there was no significant differences in the number of neutrophils between STAT6 decoy ODN-transfected mice and positive control or scrambled decoy ODN-transfected mice in

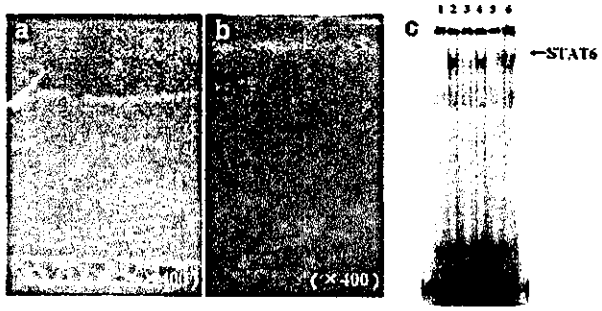

Figure 2 (a, b) In vivo distribution of fluorescein isothiocyanate (FITC)-labeled STAT6 decoy ODN in the challenged skin transfected by subcutaneous injection. FITC-labeled STAT6 decoy ODN with HVJ-E (50 μl, 20 μM) (a) or STAT6 decoy ODN was transfected into the BALB/c mouse skin by the subcutaneous injection on the day before the last challenge. It is noteworthy that the introduced FITC-labeled STAT6 decoy ODN was more localized in the dermal cells (a) than the control skins transfected with the empty envelope (b). (c) Gel mobility-shift assay for the STAT6 binding site from ear tissues specimens. Lane 1, Nuclear extract from ear tissue without last challenge (negative control), incubated with ^{32}P-labeled STAT6 oligonucleotide (ODN); lane 2, nuclear extract from challenged ear tissue (positive control), incubated with ^{32}P-labeled STAT6; lane 3, nuclear extract from challenged ear tissue-transfected STAT6 decoy ODN on the day before last challenge, incubated with ^{32}P-labeled STAT6; lane 4, nuclear extract from challenged ear tissue-transfected scrambled decoy ODN on the day before last challenge, incubated with ^{32}P-labeled STAT6; lanes 5 and 6, nuclear extract from challenged ear tissue, incubated with cold STAT6 probe (lane 5) and antibodies against STAT6 (lane 6). These results represent the findings of three independent experiments.

both acute (d) and chronic (e) CHS. In acute (d) and chronic (e) CHS, both the total number of mast cells and degranulated mast cells were reduced by transfection of STAT6 decoy ODN.

Local production of cytokines and the serum IgE level in the mice treated with or without STAT6 decoy ODN

In the supernatant from skin tissue specimens in TNCB-challenged mice, the levels of IL-4 were significantly higher than those in the supernatants from olive oil-challenged mice in both acute (Figure 5a) and chronic (Figure 5b) CHS. In contrast, the IL-4 levels in the supernatant from TNCB-challenged mice treated with STAT6 decoy ODN transfection decreased in both acute and chronic CHS (Figure 5a, b). The levels of IFN-γ in the mice with STAT6 transfection were comparable to those in the nontransfected or scrambled decoy ODN-transfected mice in both acute (Figure 5c) and chronic (Figure 5d) CHS. Furthermore, not only, the IL-4 levels which is one of representative Th2 cytokine levels, but also the IL-6 (Figure 5e, f) and eotaxin (Figure 5g, h) levels in the supernatant from skin tissue specimens obtained from STAT6 decoy ODN-transfected mice decreased in both acute (Figure 5e, g) and chronic (Figure 5f, h) CHS. The serum IgE level did not decrease by the transfection of STAT6 decoy ODN with HVJ-E in comparison to the results obtained with positive control and scrambled decoy ODN with HVJ-E in both acute (i) and chronic (j) CHS to TNCB.

Discussion

CHS is thought to be dependent on Th1 cells[1,2] although IL-4 has also been demonstrated to be involved in the response of CHS.[5-7] It has also been reported that Th2 cells in mouse skin can induce a cellular inflammatory response with faster kinetics.[24] To clarify this question, we recently established STAT6-deficient mice and concluded that STAT6 plays a central role in the induction of CHS.[10]

Furthermore, recent *in vivo* studies have demonstrated that many immune responses start predominantly as a Th1 to a Th2 response.[25,26] In line with these studies, the CHS response has also been demonstrated to start predominantly as a Th1 to a Th2 response. We, herein, examined the role of STAT6 in the induction of a response by repeated elicitation of CHS. We confirmed that the repeated elicitation of CHS to TNCB induced a shift from the Th1 to a Th2 response in wt mice, however, in comparison with the wt control mice, the ear-swelling response in STAT6$^{-/-}$ mice significantly decreased at 6 h after the last elicitation. This reduction of the peak response induced by the repeated challenge was also observed at 1–6 h in STAT6$^{-/-}$ mice sensitized with Oxa or DNFB as the contact allergen. These data indicated that STAT6 plays a crucial role in the induction of not only the single elicitation of CHS (acute CHS), but also the repeated elicitation of CHS (chronic CHS).

These results of the response induced by a single and repeated elicitation of CHS in STAT6$^{-/-}$ mice suggested that the blocking of the STAT6 signaling can be a therapeutic approach for CHS. We thus examined whether *in vivo* treatment with the transfection of STAT6 decoy ODN with HVJ-envelope (E) after the sensitization can effectively inhibit STAT6 binding to the nucleus and the response induced by the single or repeated application to TNCB. The subcutaneous injection of STAT6 decoy ODN with HVJ-E after sensitization exhibited a significant inhibitory effect on both STAT6 binding to nucleus and the late-phase response in line with Kaneda's report.[27] A histopathological analysis revealed a tremendous reduction in both the infiltration of eosinophils, mast cells, and especially mast cell degradation in single or repeated challenged skin in STAT6 decoy ODN-transfected mice. STAT6 signaling is essential for the hapten-induced increase in Th2 cytokines production *in vivo*. The ELISA technique showed the production of protein of the Th2 cytokines (ie, IL-4), IL-6 and eotaxin to decrease in STAT6 decoy ODN-transfected mice, but not in scrambled decoy ODN-transfected mice in both acute and chronic CHS, whereas the serum IgE level was not inhibited by STAT6 decoy ODN. It was noteworthy that STAT6 decoy ODN strongly inhibited the IL-6 production in chronic CHS. These data indicated that the late-phase reaction induced by mast cells may play a major role in the pathogenesis of chronic CHS in line with the previous reports,[13,14] since IL-6 production from mast cells is dependent on STAT6 signaling in the late-phase allergic responses.[28] Recently, eotaxin has been reported to be induced by fibroblast stimulated with IL-4 through STAT6 pathway.[29,30] Eotaxin induced by fibroblasts stimulated with IL-4 may thus play a major role in the chemotaxis of eosinophils. However, since STAT6 also affects the cytokine response of other inflammatory cells, such as macrophages or T cells, the significant contribu-

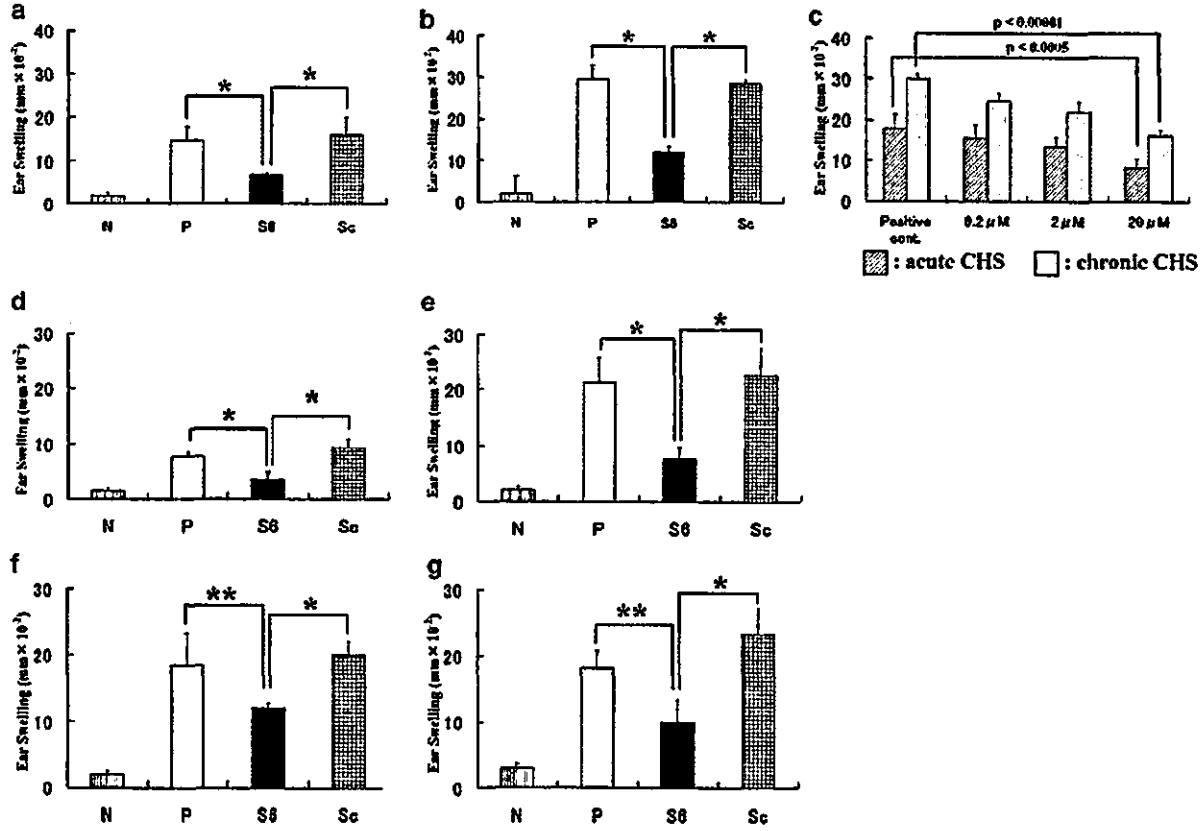

*Figure 3 Mice injected with STAT6 decoy ODN with HVJ-E exhibit a reduced CHS response to haptens. The maximal ear swelling of all groups were detected at 24 h for acute CHS and at 4 h for chronic CHS after challenge. The suppression in ear-swelling reaction was observed in both acute (a) and chronic CHS (b) to TNCB-induced CHS in the mice treated with STAT6 decoy ODN with HVJ-E. A measure of 20 μM, but not 0.2 μM, 2 μM of STAT6 decoy ODN significantly inhibited both acute and chronic CHS response in a dose-dependent manner (c). Furthermore, the CHS was induced by other haptens. Acute CHS (d, f) and chronic CHS (e, g) were induced to DNFB (d, e) and Oxa (f, g). The data presented are the mean values ± s.d. of at least five mice per group. *P<0.01, **P<0.05 significantly compared to the results of positive control or scrambled decoy ODN with HVJ-E. These results represent the findings of three independent experiments. N: negative control, P: positive control, S6: STAT6 decoy ODN with HVJ-E, Sc: scrambled decoy ODN with HVJ-E.*

tion of cells other than mast cells in late-phase allergic response might be inhibited by STAT6 decoy ODN. These data indicated that the STAT6 signal is essential in the production of Th2 cytokine, chemokine for eosinophils and the activation of mast cells.

In summary, (1) STAT6 is essential in the induction of both acute and chronic CHS. (2) STAT6 mediates the ear-swelling response induced by single and repeated elicitation via its pivotal role in Th2 differentiation thus resulting in the subsequent stimulation of IgE synthesis and eosinophils infiltration in the skin. (3) *In vitro* experiments have demonstrated that STAT6 decoy ODN selectively inhibited the expression of targeted cytokine genes (IL-4, IL-6, and eotaxin). (4) The administration of STAT6 decoy ODN markedly inhibited the antigen-specific response induced by single and repeated elicitation in CHS. (5) The inhibition of the response in acute and chronic CHS by STAT6 decoy ODN delivered by the subcutaneous administration was observed. (6) The decrease in the number of eosinophils, mononuclear cells, mast cells, and degranulated mast cells seemed to be associated with the decreased production of IL-4 and IL-6. In addition, this study demonstrated that the transcriptional factor, STAT6, is one of the key regulators promoting IgE-mediated late-phase reaction. Although a number of important issues, such as safety and side effects, have not yet been addressed in this study, the decoy strategy against STAT6 may be useful as a new therapeutic modality as gene therapy against contact dermatitis and atopic dermatitis. Since STAT6 has been postulated to play an important role in the pathogenesis of numerous diseases, for example, atopic asthma and allergic rhinitis, the development of STAT6 decoy strategy may also provide useful therapeutic tool for treating these diseases.

Materials and methods

Animals

C57BL/6 mice with a targeted disruption of the gene encoding STAT6 (STAT6$^{-/-}$) were generated in the Department of Biochemistry at the Hyogo College of Medicine as previously reported,[9] and age-matched wild-type (WT) littermate controls (C57BL/6 and BALB/c mice) were purchased from Oriental Yeast Co Ltd (Shizuoka, Japan). All animals were maintained in specific pathogen-free facilities at the Tokyo Medical and

Dental University Postgraduate School animal facilities in accordance with institutional guidelines, and all mice had free access to a commercial diet and water. They were used at 8–10 weeks of age. Each experimental group consisted of at least five mice.

Contact sensitizing reagents

The following reagents were obtained from commercial sources; 2,4,6-trinitro-1-chlorobenzene (TNCB) and 2,4-dinitrofluorobenzene (DNFB) from Nacalai Tesque, Inc. (Kyoto, Japan); 4-ethoxyl methylene-2-phenyl-2-oxazol-5-one (Oxa) from the Sigma Chemical Co. (St Louis, MO, USA).

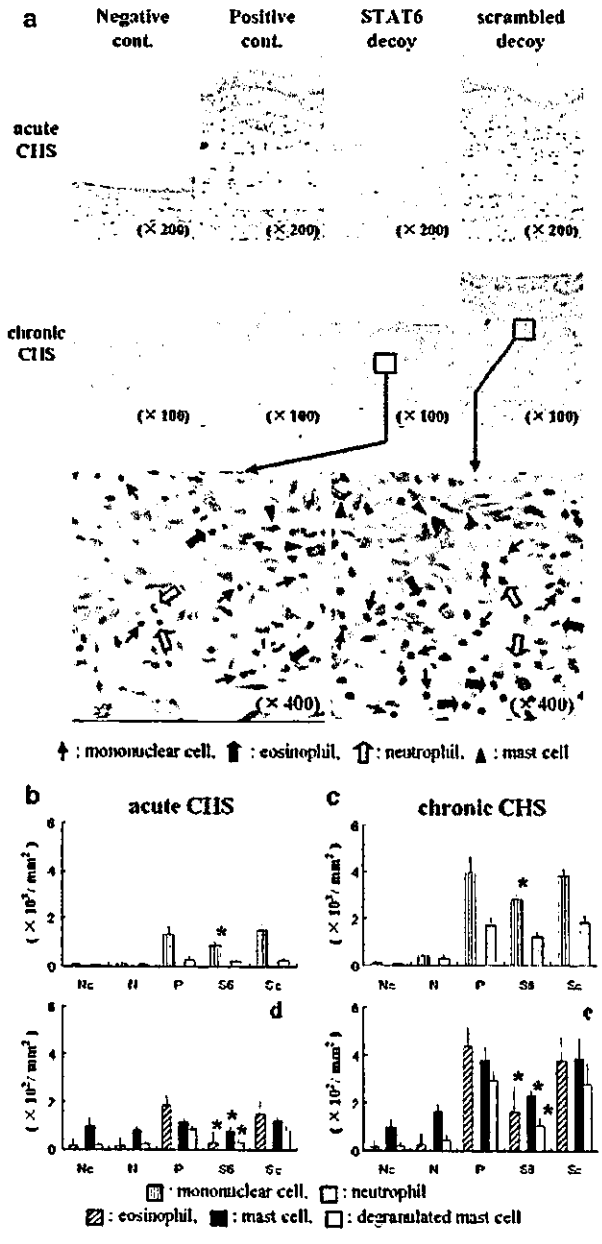

Immunization for induction of CHS to TNCB, DNFB, and Oxa

All mice were sensitized by two daily consecutive topical epicutaneous applications of 50 μl of 5% TNCB solutions, 0.5% DNFB solutions, and 3% Oxa solutions in acetone in olive oil (4:1) to the shaved abdominal skin, as described previously.[10]

Elicitation and quantitation

At 3 days after the last abdominal application, the mice were challenged by applying 20 μl of hapten solution (1% TNCB, 0.2% DNFB, or 0.5% Oxa in olive oil in acetone (4:1)) or vehicle (without TNCB, DNFB, or Oxa) on both sides of the ear lobe for the first elicitation (day 4). These groups of mice were categorized to acute CHS. Thereafter, in order to produce the chronic CHS model, the same solutions were applied 12 times to the same skin site every other day. The thickness of the ear was then measured with an engineer's micrometer (peacock; OZAKI MFG. Co., Ltd., Tokyo) at 1, 4, 6, 12, 24, 36, 48, and 72 h after challenge. The negative control mice were treated in the same fashion without hapten at only last challenge.

The percent suppression was calculated according to the formula:

$$\text{Percent suppression} = \frac{\text{Ear swelling of wt mice} - \text{ear swelling of STAT6} -/- \text{mice}}{\text{Ear swelling of wt mice} - \text{ear swelling of negative control}}$$

(Figure 1a, b)

$$\frac{\text{Ear swelling of positive control mice} - \text{ear swelling of STAT6 decoy transfected mice}}{\text{Ear swelling of positive control mice} - \text{ear swelling of negative control mice}}$$

(Figure 3)

Figure 4 (a) Histopathological findings of acute/chronic CHS in the mice transfected with STAT6 decoy ODN or scrambled decoy ODN. Acute CHS, three days after immunization, the mice were then challenged by applying 1% TNCB solution. Histologic features of 24 h CHS ear skin reaction challenged with TNCB in mice stained with HE. An extremely large degree of edema was detected in the TNCB-challenged skin in the mice treated with scrambled decoy, but not in the mice treated with STAT6 decoy. Chronic CHS, after immunization, the mice were then challenged by applying 1% TNCB solution repeatedly. Histologic features of 4 h CHS ear skin reaction challenged with TNCB in mice stained with HE solution. The ear skin reaction were observed to be the same in comparison with acute CHS. Under large magnification, stained with Giemsa's solution, a strong infiltration of mononuclear cells, neutrophils, eosinophils, mast cells, and especially degranulated mast cells was observed in the dermis of scrambled decoy ODN-transfected mice than STAT6 decoy ODN-transfected mice. (b–e) Effect of transfection of STAT6 decoy ODN on the cellular distribution of challenged skin. Profile of infiltrated cells in the challenged skin of BALB/c mice was evaluated by Giemsa stain. Challenged skin was obtained from mice pretreated with STAT6 decoy ODN or scrambled decoy ODN after being challenged with the elicitation of 1% TNCB. The columns represent the number of mononuclear cells, neutrophils, eosinophils, mast cells and degranulated mast cells in the challenged skin. The data presented are the mean values ± s.d. of at least five mice per group. These results represent the findings of three independent experiments. Nc: normal control, N: negative control, P: positive control, S6: STAT6 decoy ODN, Sc: scrambled decoy ODN.

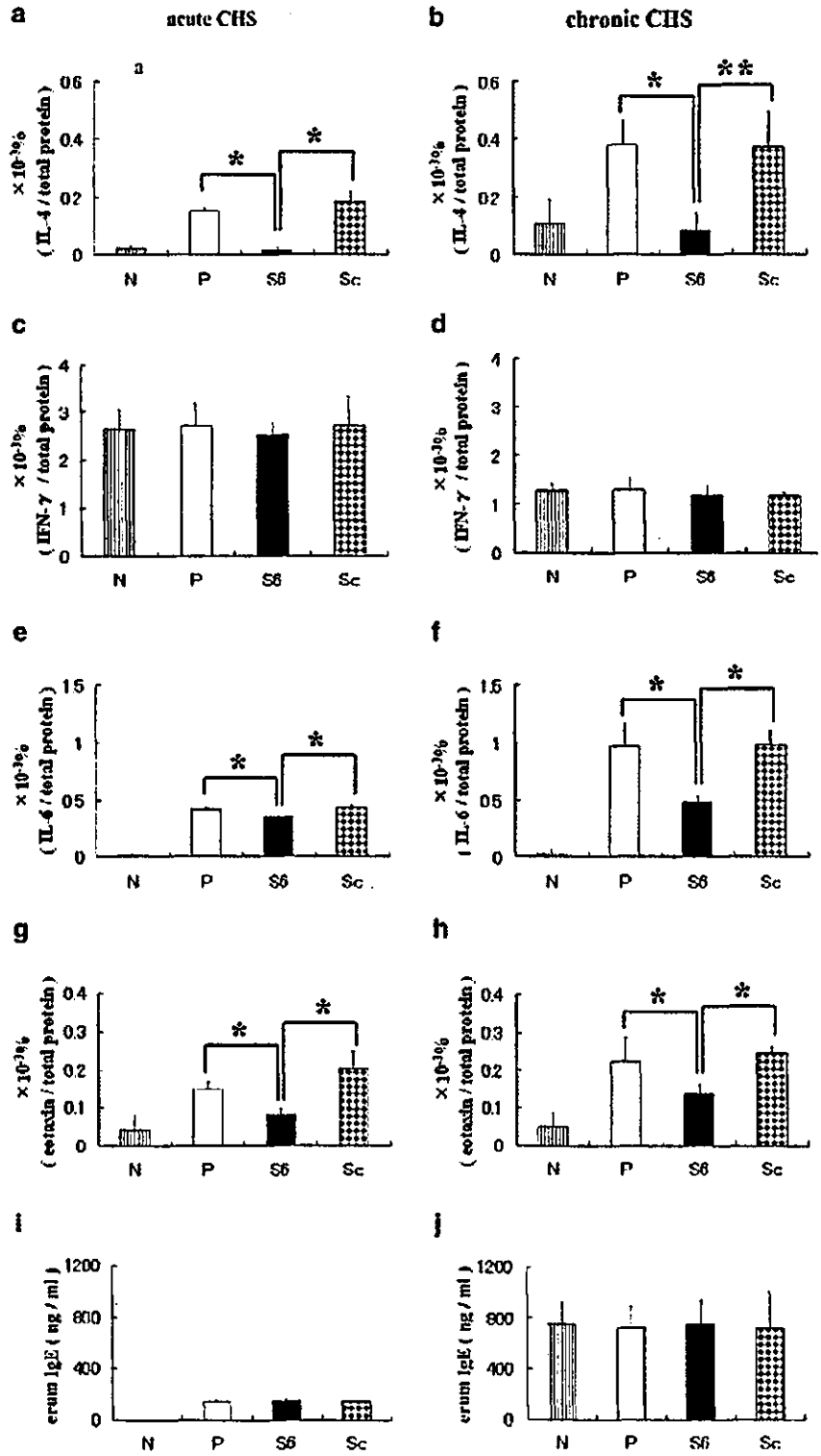

*Figure 5 Cytokine levels in the skin tissue extract and serum IgE level by ELISA assay. The cytokine levels in the TNCB-challenged skin supernatants of IL-4 (a, b), IFN-γ (c, d), eotaxin (e, f), and IL-6 (g, h) in both acute (a, c, e, g) and chronic (b, d, f, h) CHS were presented. In addition, the production of serum IgE was not affected by STAT6 decoy ODN in both acute (i) and chronic CHS (j). These data represent the mean ± s.d. for groups of four mice and are representative of three independent experiments. *P <0.01, **P <0.05 significantly compared with the cytokine levels of the positive control or scrambled decoy ODN with HVJ-E. These results represent the findings of three independent experiments. N: negative control, P: positive control, S6: STAT6 decoy ODN, Sc: scrambled decoy ODN.*

Synthesis of ODN and selection of target sequences

Sequences of the phosphorothioate ODN utilized were as follows:[31]

STAT6 decoy ODN:
5′-GATCAAGACCTTTTCCCAAGAAATCTAT-3′
3′-ATAGATTTCTTGGGAAAAGGTCTTGATC-5′
Scrambled decoy ODN:
5′-CGAAAATTCGTTAAATCACTAGCTTACC-3′
3′-GGTAAGCTAGTGATTTAACGAATTTTCG-5′

The STAT6 decoy ODN is a double-stranded phosphorothioate 28-mer that exhibits a high sequence-specific binding affinity to the transcription factor STAT6. Synthetic ODNs were dissolved in sterile Tris-EDTA buffer (10 mM Tris, 1 mM EDTA pH 8.0), purified by high-performance liquid chromatography and quantitated by spectrophotometry. Each pair of single-stranded ODN was annealed for 3 h, during which time, the temperature was reduced from 90 to 25°C. These decoy ODNs were then stored at −20°C until use.

Preparation of the HVJ-E vector

HVJ (also known as Sendai virus) was amplified as described previously.[27] The virus was inactivated by β-propiolactone (0.0075–0.001%) treatment or by UV irradiation. In both cases, the virus preparation lost the ability to replicate. The aliquots of the virus (3×10^{10} particles/1.5 μl tube) were centrifuged (18 500 *g*, 15 min) at 4°C, and the viral pellet was stored at −20°C.[27]

The inactivated virus suspension (10 000 haemagglutinating activity units (HAU)) was mixed with STAT6 decoy OND or scrambled decoy ODN (800 μg of DNA), 8 μl of 3% Triton/TE and balanced salt solution (BSS;10 nM Tris-HCl (pH 7.5), 137 mM NaCl and 5.4 mM KCl)) to yield a final volume of 100 μl. The mixture was centrifuged at 18 500 *g* for 15 min at 4°C. After the pellet was washed with 1 ml of human tubal fluid (HTF) medium (Nippon Medical & Chemical Instrument Co. Ltd, Osaka, Japan) to remove the detergent and unincorporated DNA, the envelope vector was suspended in 250 μl of HTF medium. Approximately 15–20% of DNA was incorporated into the vector. The HVJ-E vector was stored at 4°C until use. HVJ-E vector is also commercially available from Ishihara Sangyo Co. Ltd (Osaka, Japan).

In vivo transfer of ODN and FITC-labeled ODN

FITC was used to label the 5′-ends of STAT6 decoy ODN and Scrambled decoy ODN. These ODNs were injected to ear lobe subcutaneously at one day before the last challenge; in a word, in the case of acute CHS, ODNs were injected on day 4, and, in that of chronic CHS, on day 26. After transfection, the mice were killed, and ears were removed. Next, the sections were examined by fluorescent microscopy.

Electrophoretic mobility-shift assays (EMSA)

As previously described,[32] the mouse ear lobe was homogenized in 500 μl of ice-cold homogenization buffer (10 mM HEPES, pH 7.5, 0.5 M sucrose, 0.5 mM spermidine, 0.15 mM spermine, 5 mM EDTA, 0.25 M EGTA, 7 mM β-mercaptoethanol, and 1 mM phenylmethylsulfonyl fluoride) containing 0.1% Nonidet P-40. The samples were then centrifuged at 14 000 rpm for 30 min at 4°C, and the pellet nucleus was washed twice with ice-cold buffer containing 0.35 M sucrose.

After washing, the nucleus was extracted with 500 μl of ice-cold homogenization buffer containing 0.05 M NaCl and 10% glycerol for 15 min at 4°C, followed by a further extraction with homogenization buffer containing 0.3 M NaCl and 10% glycerol for 1 h at 4°C. After centrifugation at 15 000 rpm for 30 min at 4°C, the pellet was dissolved with homogenization buffer containing 0.35 M sucrose to obtain the concentration of DNA at 1 mg/ml. Then, the samples were stored in aliquots at −80°C.

After preincubation with 2 μg poly(dI-dC) as non-specific competiter DNA, 2 μl sample of the crude nuclear extract were incubated in a binding buffer containing 1 mM dithiothreitol, 1 mM phenylmethylsulfonyl fluoride, 20 μg/ml aprotinin, and 10 μl/ml leupeptin with approximately 10 000 cpm of annealed ^{32}P-labeled probe for 30 min at room temperature. The sequence of the probe for STAT5/6 was 5′-GTA TTT CCC AGA AAA GGA AC-3′ (Santa Cruz Biotechnology Inc.). The sequence of the mutant STAT6 probe was 5′-GTA TTT CGG TTA AAA GGA AC-3′. The binding reaction mixtures were separated from free oligonucleotide probes by electrophoresis on a native 5% (w/v) gel as described.[33] The reaction mixture was subjected to electrophoresis as previously described and thereafter the gels were dried and autoradiographed.

Histological examination

The ear skin specimens were excised and fixed in 10% formalin, and then were processed and stained with hematoxylin and eosin (HE), or May–Grunwald–Giemsa. The number of mononuclear cells, mast cells, and eosinophils infiltrating into the dermis was evaluated under light microscopy. The section was examined at a magnification of × 400. At least 20 fields were examined for each lobe. The number of cells was counted and expressed as the number of cells per mm^2.

Quantification of cytokine levels in skin tissue extracts

Samples of the ear extracts for ELISA were prepared as described by Ferguson *et al*.[34] Briefly, at 24 h after application of TNCB (acute CHS) and at 4 h after application of TNCB (chronic CHS), the ears were excised and immediately homogenized with 1 cm^3 of 0.1% Tween-20 in PBS. The samples were quickly frozen in liquid nitrogen, thawed in a 37°C water bath, sonicated for 15 s, and centrifuged for 5 min at 13 000 *g*, and supernatants were used as samples for ELISA. The supernatants were stored at −80°C. First, we measured the total protein levels in the supernatants with Protein Assay® (BIO-RAD, Hercules, CA, USA) according to the manufacturer's instructions. Second, the ELISA assays for IL-4, IFN-γ, IL-6, and eotaxin were conducted using ELISA kits (IL-4, IFN-γ, IL-6: Pierce Endogen, Rockford, IL, USA; eotaxin: TECHNE Corporation, Minneapolis, MN, USA) according to the manufacturer's instructions. The ratios of these cytokine levels in total protein level were examined.

Statistical analysis

The experimental data are expressed as the mean±s.d. (standard deviation) and shown in the figures as the mean+s.d. for clarity. The statistical analysis was performed using Student's *t*-test.

Acknowledgements

We thank Ms Motoko Sekiya for her excellent technical assistance.

References

1 Xu H, DiIulio NA, Fairchild RL. T cell populations primed by hapten sensitization in contact sensitivity are distinguished by polarized patterns of cytokine production: interferon gamma-producing (Tc1) effector CD8+ T cells and interleukin (IL)-4/IL-10-producing (Th2) negative regulatory CD4+ T cells. *J Exp Med* 1996; 183: 1001–1012.
2 Steinbrink K, Sorg C, Macher E. Low zone tolerance to contact allergens in mice: a functional role for CD8+ T helper type 2 cells. *J Exp Med* 1996; 183: 759–768.
3 Gautam SC, Chikkala NF, Hamilton TA. Anti-inflammatory action of IL-4. Negative regulation of contact sensitivity to trinitrochlorobenzene. *J Immunol* 1992; 148: 1411–1415.
4 Asada H, Linton J, Katz SL Cytokine gene expression during the elicitation phase of contact sensitivity: regulation by endogeneous IL-4. *J Invest Dermatol* 1997; 108: 406–411.
5 Dieli F *et al.* IL-4 is essential for the systemic transfer of delayed hypersensitivity by T cell lines. Role of gamma/delta cells. *J Immunol* 1994; 152: 2698–2704.
6 Salerno A *et al.* IL-4 is a critical cytokine in contact sensitivity. *Immunology* 1995; 84: 404–409.
7 Asherson GL *et al.* Role of IL-4 in delayed type hypersensitivity. *Clin Exp Immunol* 1996; 103: 1–4.
8 Weigmann B *et al.* Diminished contact hypersensitivity response in IL-4 deficient mice at a late phase of the elicitation reaction. *Scand J Immunol* 1997; 45: 308–314.
9 Takeda K *et al.* Essential role of Stat6 in IL-4 signaling. *Nature* 1996; 380: 627–630.
10 Yokozeki H *et al.* Signal transducer and activator of transcription 6 is essential in the induction of contact hypersensitivity. *J Exp Med* 2000; 191: 995–1004.
11 Yokozeki H *et al.* Gammadelta T cells assist alphabeta T cells in the adoptive transfer of contact hypersensitivity to para-phenylenediamine. *Clin Exp Immunol* 2001; 125: 351–359.
12 Yokozeki H *et al.* Th2 cytokines, IgE and mast cells play a crucial role in the induction of para-phenylenediamine-induced contact hypersensitivity in mice. *Clin Exp Immunol* 2003; 132: 385–392.
13 Kitagaki H *et al.* Immediate-type hypersensitivity response followed by a late reaction is induced by repeated epicutaneous application of contact sensitizing agents in mice. *J Invest Dermatol* 1995; 105: 749–755.
14 Kitagaki H *et al.* Repeated elicitation of contact hypersensitivity induces a shift in cutaneous cytokine milieu from a T helper cell type 1 to a T helper cell type 2 profile. *J Immunol* 1997; 159: 2484–2491.
15 Morishita R *et al.* Application of transcription factor 'decoy' strategy as means of gene therapy and study of gene expression in cardiovascular disease. *Circ Res* 1998; 82: 1023–1028.
16 Morishita R, Aoki M, Kaneda Y. Oligonucleotides-based gene therapy for cardiovascular disease: are oligonucleotide therapeutics novel cardiovascular drugs? *Curr Drug Targets* 2000; 1: 15–23.
17 Morishita R *et al.* *In vivo* transfection of *cis*-element 'decoy' against nuclear factor-kappaB binding site prevents myocardial infarction. *Nat Med* 1997; 3: 894–899.
18 Tomita T *et al.* Suppressed severity of collagen-induced arthritis by *in vivo* transfection of nuclear factor kappaB decoy oligodeoxynucleotides as a gene therapy. *Arthritis Rheum* 1999; 42: 2532–2542.
19 Kawamura I *et al.* Intratumoral injection of oligonucleotides to the NF kappaB binding site inhibits cachexia in a mouse tumor model. *Gene Therapy* 1999; 6: 91–97.
20 Tomita N *et al.* *In vivo* administration of a nuclear transcription factor-kappaB decoy suppresses experimental crescentic glomerulonephritis. *J Am Soc Nephrol* 2000; 11: 1244–1252.
21 Kawamura I *et al.* Intravenous injection of oligodeoxynucleotides to the NF-kappaB binding site inhibits hepatic metastasis of M5076 reticulosarcoma in mice. *Gene Therapy* 2001; 8: 905–912.
22 Abeyama K *et al.* A role of NF-kappaB-dependent gene transactivation in sunburn. *J Clin Invest* 2000; 105: 1751–1759.
23 Nakamura H *et al.* Prevention and regression of atopic dermatitis by ointment containing NF-kB decoy oligodeoxynucleotides in NC/Nga atopic mouse model. *Gene Therapy* 2002; 9: 1221–1229.
24 Muller KM *et al.* Th2 cells mediate IL-4-dependent local tissue inflammation. *J Immunol* 1993; 150: 5576–5584.
25 Garside P, Mowat AM. Polarization of Th-cell responses: a phylogenetic consequence of nonspecific immune defence? *Immunol Today* 1995; 16: 220–223.
26 Swain SL. Generation and *in vivo* persistence of polarized Th 1 and Th 2 memory cells. *Immunity* 1994; 1: 543–552.
27 Kaneda Y *et al.* Hemagglutinating virus of Japan (HVJ) envelope vector as a versatile gene delivery system. *Mol Ther* 2002; 6: 219–226.
28 Malaviya R, Uckun FM. Role of STAT6 in IgE receptor/FcepsilonRI-mediated late phase allegic responses of mast cells. *J Immunol* 2002; 168: 421–426.
29 Hoeck J, Woisetschlager M. Activation of eotaxin-3/CCLI26 gene expression in human dermal fibroblasts is mediated by STAT6. *J Immunol* 2001; 167: 3216–3222.
30 Hoeck J, Woisetschlager M. STAT6 mediates eotaxin-1 expression in IL-4 or TNF-alpha-induced fibroblasts. *J Immunol* 2001; 166: 4507–4515.
31 Wang LH *et al.* Targeted disruption of stat6 DNA binding activity by an oligonucleotide decoy blocks IL-4-deriven T(H)2 cell response. *Blood* 2000; 95: 1249–1257.
32 Molitor JA *et al.* NF-kappaB. A family of inducible and differentially expressed enhancer-binding proteins in human T cells. *Proc Natl Acad Sci USA* 1990; 87: 10028–10032.
33 Schreiber E *et al.* Rapid detection of octamer binding proteins with 'mini-extracts', prepared from a small number of cells. *Nucleic Acids Res* 1989; 17: 6419.
34 Ferguson TA, Dube P, Griffith TS. Regulation of contact hypersensitivity by interleukin 10. *J Exp Med* 1994; 179: 1597–1604.

Available online at www.sciencedirect.com
SCIENCE DIRECT
Clinical Immunology 112 (2004) 92–105
CLINICAL IMMUNOLOGY
www.elsevier.com/locate/yclim

Hemagglutinating virus of Japan protein is efficient for induction of $CD4^+$ T-cell response by a hepatitis B core particle-based HIV vaccine

Satoshi Takeda,[a] Kouichi Shiosaki,[b] Yasufumi Kaneda,[c] Tetsuya Nakasatomi,[a] Hitomi Yoshizaki,[a] Kenji Someya,[a] Yusuke Konno,[c] Yasuyuki Eda,[b] Youichirou Kino,[b] Naoki Yamamoto,[a] and Mitsuo Honda[a,*]

[a] *AIDS Research Center, National Institute of Infectious Diseases, Tokyo 162-8640, Japan*
[b] *The Chemo-Sero-Therapeutic Research Institute, Kumamoto 869-1298, Japan*
[c] *Division of Gene Therapy Science, Osaka University School of Medicine, Osaka 565-0871, Japan*

Received 10 June 2003; accepted with revision 5 April 2004

Abstract

By using the hepatitis B core (HBc) protein gene as a carrier, HIV-1 *env V3* gene was inserted into the carrier gene, and the HIV gene was expressed inside a chimeric HIV-HBc particle (HIV-HBc), which was a unique candidate for induction of HIV-specific CTL activity. This was seen significantly in mice without the need of an adjuvant, because other responses specific for the HIV peptide such as T-cell proliferation and antibody production were not induced. However, when hemagglutinating virus of Japan (HVJ) protein was incorporated into an anionic liposome containing HIV peptide (HIV-HVJ-liposome) and was used as a booster immunization in HIV-HBc primed animals, the HIV-specific T-cell response and enhanced CTL activity were clearly induced in consecutively immunized animals. Furthermore, the HIV-specific humoral immune response was also induced and a neutralization activity was detected in the immune sera. Thus, when an HIV peptide antigen is expressed inside the virus like a particle of HBc, it can induce both cellular and humoral immunities when an HVJ-HIV-liposome, but not an HIV-liposome, is inoculated as the booster antigen. The HVJ-stimulated splenocytes secreted IL-18 and IL-12 to synergistically enhance the secretion of IFN-γ in vitro. These findings suggest that the HVJ protein is effective at inducing the HIV-specific immunities, if used as part of a booster antigen in the consecutive immunization regimen.

Keywords: HVJ protein-incorporated liposome; HIV-hepatitis B core chimeric protein; HIV-specific immunity; Synergy of IL-18 and -12 to secrete IFN-γ

Introduction

A variety of novel approaches are currently being investigated to promote effective immunity against HIV-1. Such approaches often include attenuated, recombinant bacterial vectors that express antigenic epitopes from those of HIV [1–4], recombinant adenovirus vectors [5], recombinant vaccinia virus [6], DNA vaccines expressing gp120 [7], and synthetic peptides containing T- and B-cell epitopes of HIV as immunogens [8,9]. These candidate vaccines rely on the induction of both cellular and humoral immunities. It has been suggested that such immunities help protect individuals from HIV infection and from the subsequent development of AIDS [10]. Furthermore, HIV-specific $CD4^+$ T-cell response may play a critical role in vaccine development and immunother-

Abbreviations: HVJ, hemagglutinating virus of Japan; HBc, hepatitis B core protein; HIV-HBc, chimeric HIV-V3-HBc particle; HVJ-liposome, liposome with incorporated HVJ protein; HIV-liposome, liposome which encapsulated circular HIV-V3 peptide; HIV-HVJ-liposome, HVJ-liposome which encapsulated HIV-V3 circular peptide; HIV_{HXB2}-HVJ-liposome, HVJ-liposome encapsulated circular HIV-1_{HXB2} V3 peptide; V3, principal neutralizing determinant; KLH, keyhole limpet hemocyanin; KLH-IIIB, KLH-conjugated HIV-1_{HXB2} V3 peptide; BSA-IIIB, BSA-conjugated HIV-1_{HXB2} V3 peptide; Chol, Cholesterol; PC, phosphatidylcholine; Sph, shingomyelin; DOPE, dioleoylphosphatidylethanolamine; DC-chol, dimethylaminoethane carbamoyl-cholesterol; HAU, hemagglutinating unit; SI, stimulation index.

* Corresponding author. AIDS Research Center, National Institute of Infectious Diseases, 1-23-1 Toyama, Shinjuku-ku, Tokyo 162-8640, Japan. Fax: +81-3-5285-1183.
E-mail address: mhonda@nih.go.jp (M. Honda).

1521-6616/$ - see front matter © 2004 Elsevier Inc. All rights reserved.
doi:10.1016/j.clim.2004.04.001

apeutic interventions that aim to maintain effective immunity to HIV infection [11].

To render subunits of viral antigen or synthetic peptides immunogenic, a T helper cell's peptide or protein is fused to a target peptide [8,12], because free synthetic peptides or proteins are usually poor immunogens. For several reasons, the hepatitis B core (HBc) protein is a potential target carrier peptide [13–17]: (i) HBc can be assembled and can form particles that can induce immunity without the use of an adjuvant [18]. (ii) HBc Ag is a strong T-cell immunogen and is recognized over a wide range of MHC haplotypes [19]. (iii) The HBc Ag gene has been fused with respective target epitope genes to the N terminus [20–24], to the C terminus [14], and to internal sites [16,23,25,26]. In the present study, the HIV gene was inserted at the internal site of the HBc gene and the antigen was expressed inside the particles of the HBc chimeric protein (HIV-HBc) that spontaneously aggregated to a rigid particle of approximately 30 nm in diameter. This type of antigen inside the particle induced antigen-specific CTL but could not induce the antigen-specific $CD4^+$ T-cell response. These findings suggest that the HIV-HBc antigen may not be a suitable immunogen when used alone. However, the HIV-specific T-cell response is effectively inducible when the hemagglutinating virus of Japan (HVJ) protein was incorporated into anionic-type HIV-liposomes encapsulated by circular HIV-V3 peptides (HIV-HVJ-liposome). The HIV-HVJ-liposome was used as a booster injection in HIV-HBc primed animals.

In this paper, we chose the third variable domain (V3) of HIV-1 isolates' gp120 as an immunogen, because it evokes neutralizing antibody recognizing V3-tip region with a low efficiency by itself [27]. The V3 region is suggested to be immunodominant and so of importance in vaccine development [28]. The site is also assumed to be a chemokine receptor-binding site by the crystal structure analysis [29–31]. Furthermore, strong cellular immune responses and high HIV-specific neutralizing activity may account for long-term nonprogression in different individuals [32,33]. To improve immunogenicity of the V3 site for immunization of experimental animals, we designed to enhance immune induction of the HIV V3-specific immunity by using the HVJ protein-incorporated anionic liposome.

Materials and methods

Animals

Female eight-week-old BALB/c mice ($H\text{-}2^d$), and 6-week-old Hartley strain guinea pigs (400 g), were purchased from the Japan SLC Co., Ltd., Hamamatsu, Japan and were used within 10 days. All animal care and housing requirements determined by the National Institute of Infectious Diseases (NIID) committee for the care and use of laboratory animals were followed. Animal protocols were reviewed and approved by an institutional animal care and use committee.

Construction of expression vectors and preparation of HIV-HBc chimeric particles

A synthetic DNA fragment encoding 21-aa or 19-aa V3 tip sequence of HIV-1_{HXB2} or HIV-1_{MN}, respectively, was inserted into plasmid pYGHBc [34], which are seen in yeast cells. The product of HIV-HBc chimeric particles were purified and prepared as a vaccine antigen by using the methods described by Shiosaki et al. [15] and Miyanohara et al. [18]; however, different oligonucleotides were used for the present study. The monoclonal antibodies used for the antigen analysis by ELISA, Western immunoblot, and immuno-electron microscopy, were anti-HBc antibody [18], anti-HIV_{HXB2} V3 mAb 0.5β [35], and anti-HIV_{MN} V3 mAb μ5.5 [36].

Preparation of both anionic and cationic HIV-HVJ-liposomes

Lipids

Cholesterol (Chol), egg yolk phosphatidylcholine (PC), and egg yolk sphingomyelin (Sph) were purchased from Sigma (St. Louis, MO). Bovine brain phosphatidylserine (PS) was purchased from Avanti Polar Lipids Inc. (Birmingham, AL). Dioleoylphosphatidylethanolamine (DOPE) and dimethylaminoethane carbamoyl-cholesterol (DC-chol) were obtained from NOF Corporation (Tsukuba, Ibaraki, Japan).

Preparation of HVJ

HVJ (Z strain) was grown in chorioallantoic fluid of 10-day-old embryonated chicken eggs at 36.5 °C. HVJ was collected as a pellet by centrifugation at 27,000 × *g* for 30 min at 4 °C and was suspended with a balanced salt solution (BSS; 10 mM Tris–HCl pH 7.5, 137 mM NaCl, 5.4 mM KCl). RNA genome of HVJ was inactivated by UV irradiation (198 mJ/cm^2) just before use.

Preparation of anionic-type and cationic-type liposomes

First, lipid mixtures were prepared by dissolving PC (1.63 mg), DOPE (1.53 mg), Sph (1.47 mg), and Chol (3 mg) in 0.5 ml chloroform. PS (1.25 mg) or DC-chol (0.75 mg) was added to the lipid mixtures to prepare the anionic-type or cationic-type HVJ-liposomes, respectively. The lipids in chloroform was transferred to a glass tube and dried as a thin lipid film by evaporation, as described elsewhere [37]. Both of the HIV Env V3 synthetic circular peptides; circular IIIB-V3, VEINCTRPLNNTRKSIRIQRGPGRAFVTIGSIIGDIRQAHCNLSR; and circular MN-V3, VEINCTRPNNNTRKSIHIGPGRAFYTTGSIIGDIRQAHCNLSR (1.67 mg each, Takara Shuzo Co., Ltd., Kusatsu, Shiga, Japan) were dissolved in 200 μl of distilled water. The suspension was then added to the dried lipid mixture. Liposomes were prepared by vigorous shaking, as described previously [38]. In the case of the anionic-type liposomes, they were sonicated for 3 s and 300 μl of BSS

was added to the liposomes followed by gentle shaking at 37 °C for 30 min. For cationic-type HVJ-liposomes, the liposome suspension was extruded through cellulose acetate membrane filters (pore size 0.45 μm and 0.20 μm) as described previously [39].

Preparation of HVJ-liposomes

The liposome suspension prepared above was mixed with a UV-inactivated HVJ suspension [15,000 hemagglutinating unit (HAU)] for 10 min on ice and incubated at 37 °C for 1 h while shaking the suspension in a water bath. The HVJ-liposome complexes were then separated from free HVJ by sucrose density gradient centrifugation (62,800 × *g* at 4 °C for 1.5 h). The HVJ-liposomes between BSS and 30% sucrose solution were collected. The volume of HVJ-cationic liposome was adjusted to 300 μl with BSS. The HVJ-anionic liposomes were diluted 4 times with BSS and centrifuged at 27,000 × *g* for 30 min at 4 °C. The pellets were suspended with 300 μl of BSS by vortexing.

Enzyme-linked immunosorbent assay

Peptide-based ELISA, as described previously [40], was performed to detect antigen-specific antibodies within the guinea pig.

Cytotoxicity assays

The procedure for in vitro CTL activation and in vitro effector cell assay has been described previously [28,41–43]. In brief, spleen cells were isolated from mice immunized with vaccine antigens. Primed and washed cells (1×10^7) were incubated for 6 days with 10 μg of synthetic V3 peptide per milliliter. The restimulated spleen cells were incubated for 4 h with ^{51}Cr-labeled M12.4.5 (H-2^d), BW5147 (H-2^k), and S49 (H-2^s) cell lines used as target cells. The target cells were treated with ^{51}Cr at a concentration of 100 μCi for 90 min, and were then pulsed with 10 μg of the synthetic V3 peptide for 60 min. The BW5147 (H-2^k) and S49 (H-2^s) cell lines were kindly provided by Dr. Ethan M. Shevach, National Institutes of Health, Bethesda, MD; these cells were also used as target cells. The percentage of specific release was calculated as follows: % specific release = [(experimental release − spontaneous release)/(maximum release − spontaneous release)] × 100. The sequences of synthetic peptides of HIV_{HXB2} and HIV_{MN} V3 region of envelop proteins used for effector cells induction were RIQRGPGRAFVTIGK (P18IIIB) [42] and RIHIGPGRAFYTTKN (P18MN) [42], respectively (Takara Shuzou).

T-cell proliferation assay

Lymphocyte proliferative assays were performed as previously described [44]. Briefly, isolated spleen cells were pooled and the $CD4^+$ or $CD8^+$ fraction was then depleted using magnetic cell sorting (MACS, Militenyi Biotec., Bergisch Gladbach, Germany) [40]. Results are expressed as the stimulation index (SI), which was calculated as a ratio of the counts per minute (cpm) in the presence and absence of an antigen.

PBMC-based virus neutralization assay of HIV-1

The serum antibody of the guinea pigs inoculated with HIV-HBc following a booster injection of HIV-HVJ-liposome or a booster injection of HIV-liposome was purified from the whole sera from 15 immunized guinea pigs with Protein A Sepharose (Amersham Pharmacia Biotech, AB, Uppsala, Sweden). Serum IgG from guinea pigs injected with the HIV-HVJ-liposome and normal guinea pig IgG were also purified by the same method. The diluted serum antibodies were incubated with 100 $TCID_{50}$ units of HIV-1_{LAI}, HIV-1_{MN} and HIV-1_{Th22} (AIDS Research and Reference Reagent Program, NIH, Rockville, MD). The mixtures were incubated with PHA-activated peripheral blood mononuclear cell (PBMC). After being washed three times with PBS, the cells were cultured in the presence of recombinant human IL-2 (40 units/ml, Shionogi and Co., Ltd., Osaka, Japan) for 7 days. The amount of HIV in the supernatant was measured by HIV-1 p24 antigen ELISA (Dinabot, Ltd., Tokyo, Japan) [43,45]. The in vitro neutralization activity of the immune IgG against HIV-1 was determined by using 100 $TCID_{50}$ of the stock virus [43] and was expressed as percentage inhibition of p24 antigen production in the culture supernatants compared with that of the cultures to which serum IgG from normal guinea pigs was added. For the neutralization assays, virus stocks were titrated on PHA-activated normal PBMC and the $TCID_{50}$ of each virus was determined [43,46].

Cytokine ELISAs

Specific ELISAs determined the amounts of IL-12, IL-18, and IFN-γ in culture supernatants. IL-18 ELISA kit was purchased from Fujisaki Institute, Hayashibara Biochemical Laboratories, Okayama, Japan and IL-12 and IFN-γ ELISAs from R&D Systems Inc., Minneapolis, MN.

Statistical analysis

Calculations of the geometric mean ± SD were carried out with a microcomputer. Significance was defined as $P < 0.05$.

Results

Construction of pYGHBc-HIV and preparation of HIV-HBc chimeric particles

Each V3 peptide gene from HIV-1_{HXB2} or HIV-1_{MN} was inserted into an internal position of pYGHBc (pYGHBc-

HIV) and the amino acid sequences of the V3 regions of HIV-1_{HXB2} and HIV-1_{MN} genes were as follows (name, sequence): synthetic IIIB-V3 peptide, LNNTRKSIRIQRGP-GRAFVTI; and synthetic MN-V3 peptide, PNNKRKR IHIGPGRAFYTT (Fig. 1A). Protein particles were prepared by purification from the extract of yeast cells that expressed the pYGHBc-HIV V3 as described by Shiosaki et al. [15] and Miyanohara et al. [18] to be a single protein band (upper panel of Fig. 1B). To determine the antigen capability of the purified protein particle, we analyzed whether the purified protein particle was the fusion protein of HBc and V3 peptide of HIV-1_{HXB2} by Western blot assay (lower left panel of Fig. 1B). The protein showed reactive behavior with both anti-V3 0.5β mAb and anti-HBc Yc-3 mAb (lower left and lower right panels of Fig. 1B, respectively), indicating that the protein is a chimeric protein, which is composed of HBc protein and HIV Env V3 peptide antigen of HIV-1_{HXB2}. HIV_{MN}-HBc chimeric particle was similarly prepared.

Furthermore, the HIV-HBc chimeric proteins spontaneously aggregated to form a rigid particle of approximately 30 nm in diameter. This was seen by electron microscopy and sucrose-density ultracentrifugation analysis, and was stable at 4 °C for 2 months (data not shown). The binding

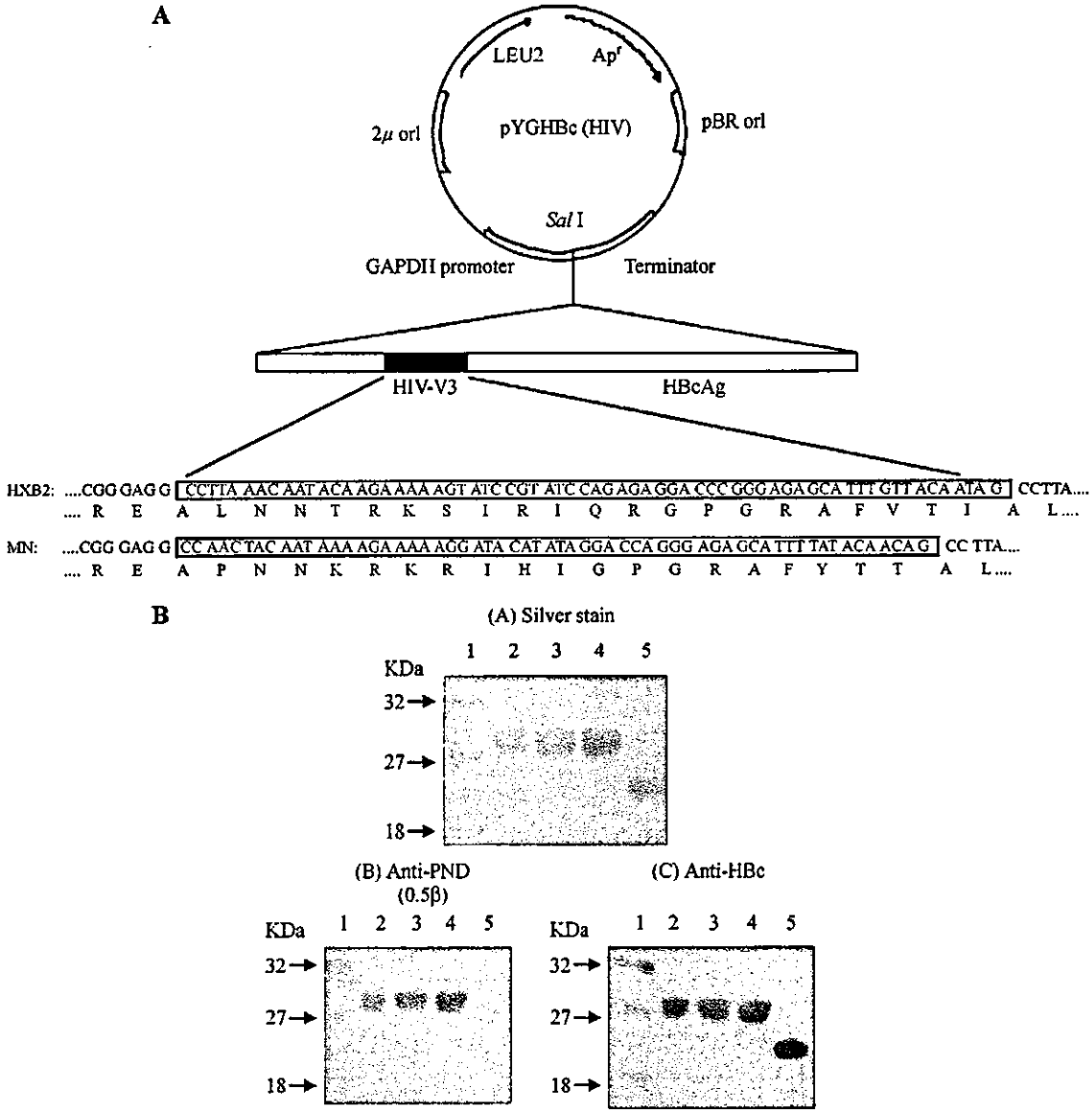

Fig. 1. Vector construction and expression of the HIV-HBc chimeric protein. (A) Vector construction of the HIV-HBc chimeric protein. DNA fragments encoding the V3-tip of the HIV V3 region from HIV-1_{HXB2}, and HIV-1_{MN} were inserted into the *SalI* restriction site in the gene for HBc antigen in plasmid pYGHBc. Apr, pBR ori, GAPDH promoter, 2μ ori, and LEU indicate genes for resistance to the drug marker, promoter, and initiation sites. DNA sequences of inserted fragments are in boxes and their deduced amino acid sequences are aligned. (B) Detection of the HIV-HBc chimeric protein by SDS-PAGE (upper panel) and Western blotting. A purified chimeric particle was separated by SDS-PAGE and detected by Western blotting with an anti-HIV Env V3 0.5β mAb or an anti-HBc Yc-3 antibody (lower left and lower right panels). Lane 1, molecular weight marker; lanes 2–4, HIV-HBc chimeric protein; lane 5, HBc protein.

ability of the HIV-HBc chimeric particle with anti-HIV_{HXB2} V3 mAb 0.5β, and anti-HIV_{MN} V3 mAb μ5.5 was examined using the ELISA antigen and immuno-electron microscopy, resulting in that the bindings were negative for anti-V3 antibodies, in contrast the binding was positive for anti-HBc antibody (data not shown). Thus, these data suggested that the HIV peptide antigens were assumed to be inside the HIV-HBc chimeric particle but not on the surface of the particle.

Experimental protocol

As shown in Fig. 2, in the first series of experiments, mice were intradermally injected in the neck with 10 μg of HIV-HBc chimeric protein within 100 μl of saline solution. The mice were given identical booster injections s.c. 7 days later. In the next series of experiments, we determined whether booster injections of the HIV-HVJ-liposome were able to elicit or enhance both cell-mediated and humoral immunity against the HIV antigen in mice and guinea pigs. Mice were immunized twice with 10 μg of HIV-HBc in saline. Two weeks later after the second immunization, the immunized animals were given an HIV-HVJ-liposome that included 10 μg of circular HIV-V3 peptides. Guinea pigs were immunized (50 μg per animal) with the HIV-HBc in saline and followed by an administration with the HVJ-liposome that included 10 μg of HIV-V3 circular peptides. As controls, the HIV-HBc-immunized animals were boosted with liposomes that had not incorporated HVJ protein but which did include 10 μg of circular HIV-V3 peptides (HIV-liposome); HBc-immunized animals were boosted with HIV-HVJ-liposome with 10 μg of circular HIV-V3 peptides. Normal animals were also injected with the HIV-HVJ-

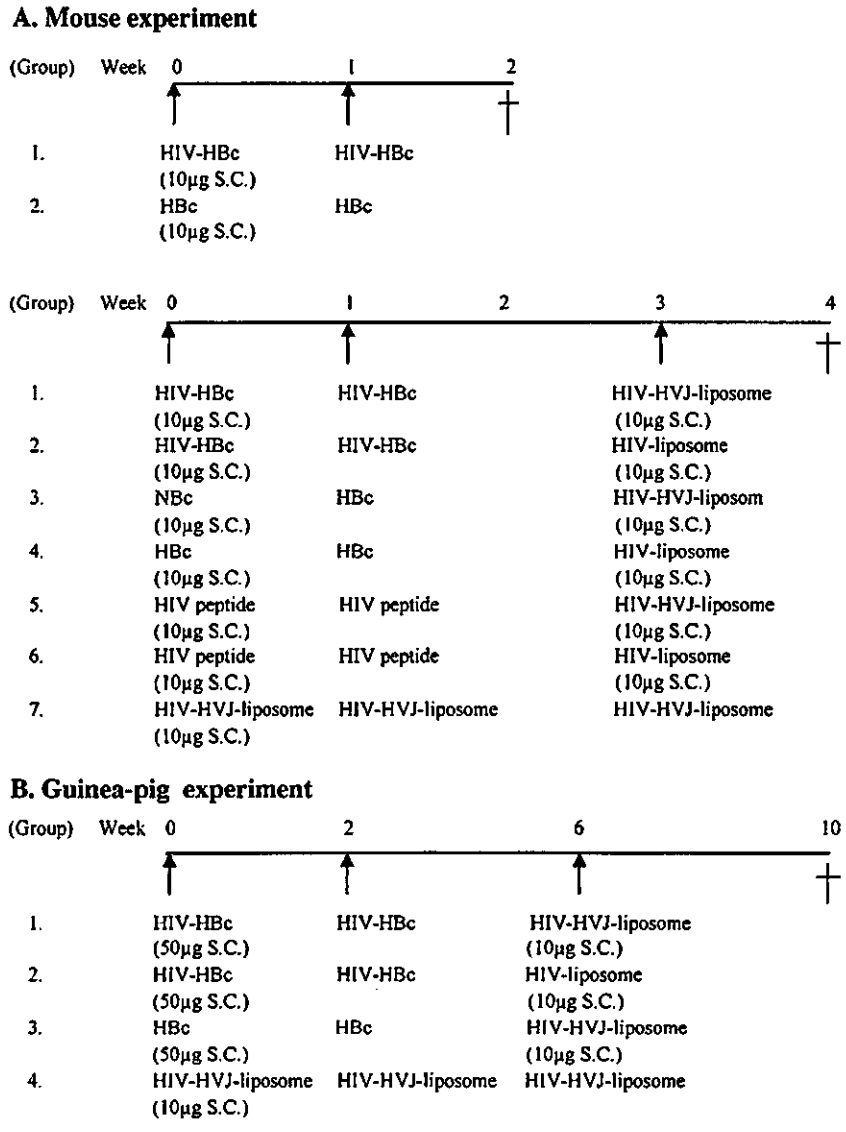

Fig. 2. Immunization schedule for induction of HIV-specific immunity.

liposome. In all experiments, five animals were used for each condition in all three of the experiments.

Characteristic immunogenicity of the HIV-HBc in mice and guinea pigs

To study the immune responses in mice, BALB/c mice were injected with an HIV-HBc chimeric protein and an HBc protein. Effector cells from the spleens of the mice immunized with HIV-HBc were generated by incubation with the V3 peptide in vitro. The stimulated effector cells significantly lysed target cells coated with the identical peptide but they did not lyse cells that were not coated (Fig. 3A). The induction of cytolytic response was specific to the HIV-antigen when it was expressed inside the chimeric protein particle; cytolytic activity was not detected when mice were immunized with an HBc protein alone and assayed for V3-specific CTL under the same condition (open triangle in Fig. 3A). Furthermore, the reactivity was restricted to the class I major histocompatibility complex, H-2^d, because cytolytic activity was not seen against allogeneic cells of BW5147 (H-2^k) and S49 (H-2^s) coated with the peptide (Fig. 3B) and the recognition of peptide 18IIIB and peptide 18MN are restricted by class I D^d molecule [28,42].

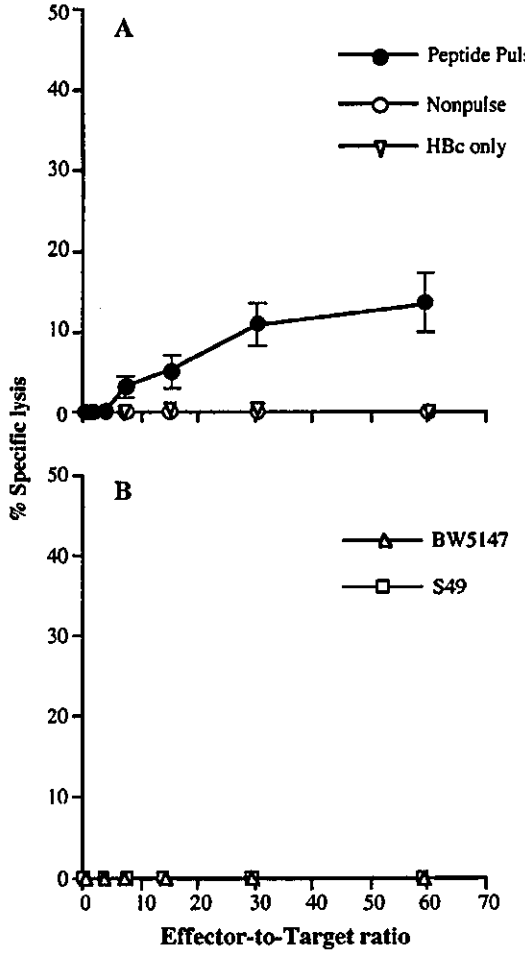

Fig. 3. Immunization of HIV-HBc chimeric antigen induces HIV-specific CTL in mice. (A) Cytolytic activity was measured against M12.4.5 target cells pulsed or not pulsed with the V3-tip peptide. The restimulated spleen cells from HIV-HBc-immunized mice were incubated with ^{51}Cr-labeled target cells that were either pretreated with the synthetic peptide (●), or untreated (○). As a control, the effector cell was prepared from HBc-immunized animals, and was incubated with ^{51}Cr-labeled target cells pretreated with the same synthetic peptide (▽). (B) Cytolysis was restricted to the major histocompatibility complex class I. Cytolysis was measured against BW5147 (△) and S49 (□).

The stimulatory effects of the HIV V3 peptide on the proliferative responses of spleen cells from the HIV-HBc immunized mice were tested 7 days after re-immunization with the same antigen. The V3 peptide stimulation did not enhance proliferations of the immune spleen cells at concentrations from 1 to 100 μg/ml, whereas HBc elicited more than 10 SI in all HIV-HBc- or HBc-immunized animals (data not shown).

Similarly, antibody titers of the sera from the above two groups specific for HIV-V3-tip antigen were all less than 10, which a value of 10 reflected an undetectable level of the antibody titer by the assay. However, HBc specific antibody titers were detected at 1:870–1150 in both groups of animals tested (data not shown).

Taken together, although these results demonstrate that immunization with a confined antigen (such as an HIV-V3 peptide expressed inside HIV-HBc particle) is able to induce HIV-specific CTL activity, neither antigen-specific $CD4^+$ T-cell nor humoral responses were observed. These results suggest that the HIV-HBc chimeric particle may induce HIV antigen-specific memory cells, but not induce effector cells effectively.

Booster injection of HVJ protein including HIV-liposome (HIV-HVJ-liposome) makes it possible to elicit $CD4^+$ T-cell response, enhanced CTL, and neutralization antibody production specific for the HIV-antigen

To study whether we could elicit marked HIV-specific immune responses to animals primed with the HIV-HBc chimeric protein, HVJ-protein was incorporated into HIV-liposome, which were used in antigen-primed animals as a booster injection. We initially characterized the effect of the incorporation of the HVJ protein into the liposome in a consecutive immunization strategy involving priming with HIV-HBc and boosting with anionic HIV_{HXB2}-HVJ-liposome. When HIV_{HXB2} V3-peptide was used, peptide-specific proliferative responses were detected with the addition of 5 μg/ml of the peptide to the culture of spleen cells from the immunized animals with the consecutive prime/boost regimen (Fig. 4). However, a lack of incorporation of the HVJ protein in HIV_{HXB2}-liposome in the booster antigen in the immunization strategy resulted in a marked decrease in the intensity of the proliferative response. In control animals that only had received a booster injection of HIV-HVJ-liposome, proliferative responses were not detected. Con A was used at a concentration of 2 μg/ml in spleen cell

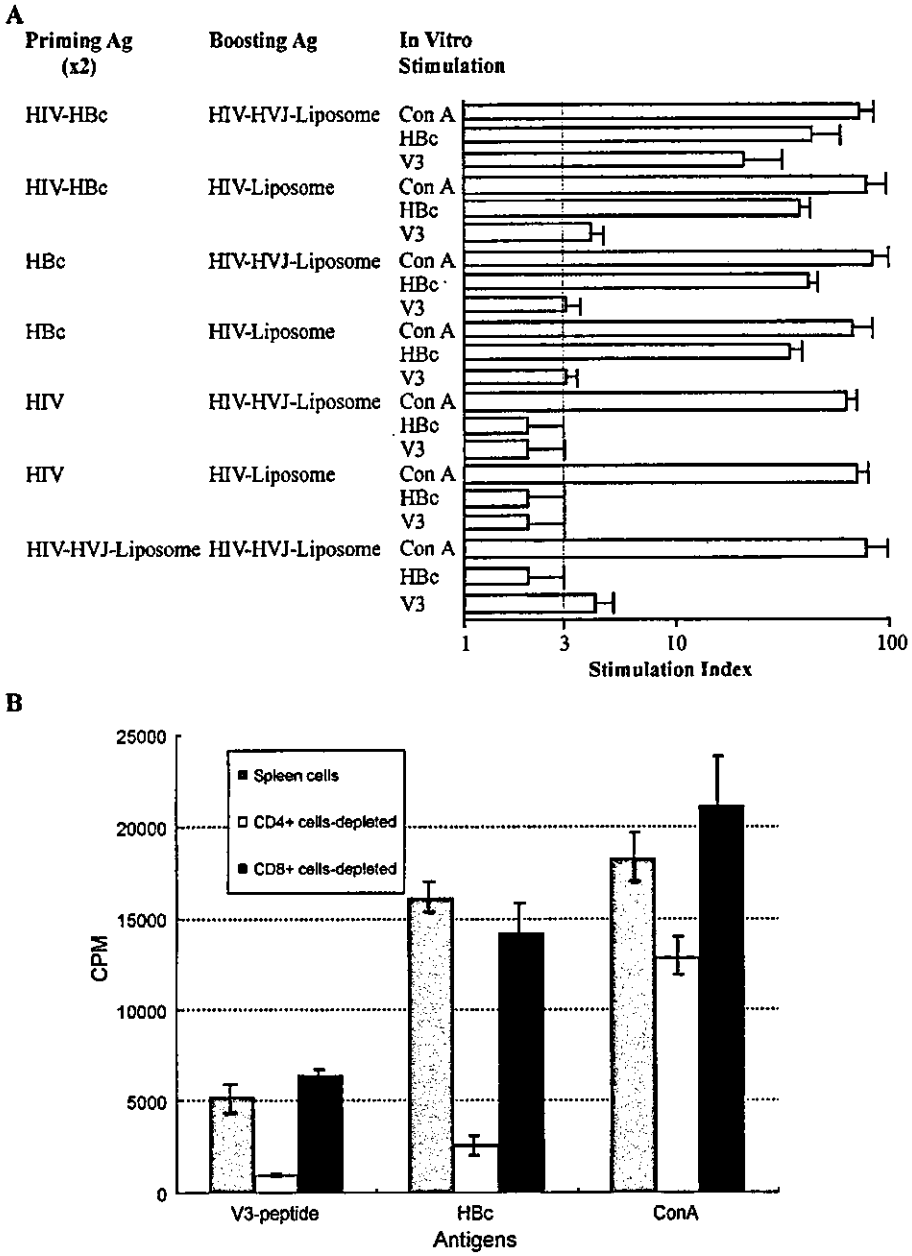

Fig. 4. $CD4^+$ T-cell proliferative responses specific for HIV-1 Env-V3 antigens. (A) The proliferative responses can be induced in animals immunized with the HIV-HVJ-liposome, which incorporated the HVJ protein into the HIV-liposome in a consecutive immunization regimen, involving priming with HIV-HBc and boosting with the HIV-HVJ-liposome. An anionic HIV-HVJ-liposome booster injection into HIV-HBc-primed guinea pigs resulted in a rise in lymphoproliferative responses to HIV-1 Env V3 antigens. The SIs of PBMC obtained from five guinea pigs in each group with various immunization regimens are shown in comparison to those obtained by stimulation with HIV-1_{HXB2} V3 circular peptide, HIV-1_{MN} V3 circular peptide, HBc protein, or medium alone. SIs are expressed as mean ± SEMs. Because results of SIs obtained by using HIV-1_{HXB2} V3 circular peptide and HIV-1_{MN} V3 circular peptide were roughly similar, the former results were shown. (B) Aliquots of spleen cells from mice vaccinated with the prime-boost regimen were depleted of $CD4^+$ or $CD8^+$ population before measuring the V3 peptide-specific proliferative responses.

cultures of normal animals and SI was always defined as more than 50. These results provide evidence that the incorporation of the HVJ protein into liposomes affects induction of a strong HIV-specific proliferative response in animals that had been immunized with the prime/boost regimen. Among the six groups, splenocytes from the mice in Group 1 (immunized with a prime-boost regimen) showed the highest levels of T-cell proliferative responses against the V3-loop peptides. The mean SI of each of the seven groups was 23.6 ± 12, 3.8 ± 2.4, 3.3 ± 1.3, 3.1 ± 1.5, 2.1 ± 1.3, 2.3 ± 1.4, and 4.4 ± 2.8, respectively (Fig. 4A). Depletion of the $CD4^+$ T-cell fraction dramatically reduced the proliferative responses from Group 1 to <10% (Fig. 4B). In contrast, proliferative activity was not affected by the depletion of the $CD8^+$ fraction from the cell suspensions.

We evaluated the effect of the anionic-type HIV-HVJ-liposome on induction of HIV-V3-specific CTL. The HIV-HVJ-liposome was administered to mice 3 weeks after immunization with HIV-HBc. CTL activity was clearly induced against syngeneic target cells pulsed with the HIV-1_{HXB2} V3 peptide (Figs. 5A and C) or HIV_{MN} V3 peptide (Figs. 5B and D) at an effector-to-target ratio from <1:6.25 in the mice inoculated with the booster injection of the HVJ-liposome that encapsulated the circular V3 peptide. However, in the booster injection of liposome that did not incorporate HVJ, the induction of HIV-specific CTL activities in the HIV-HBc primed animals was detected at an E/T ratio of 1:50–100. Furthermore, the CTL activity in the animals immunized with HVJ-HIV-liposome only was 18 ± 8.5% at 1:60 which is significantly less than that of prime-boost regimen consisting of HBc-HIV and HVJ-HIV-liposome (closed square in Figs. 5A and B). This result demonstrates that the incorporation of HVJ into liposome enhances CTL activity approximately 10-fold that of animals immunized with HVJ-unincorporated liposome (Figs. 5A and B). The enhanced induction of CTL activity by the HIV-HVJ-liposome is HIV-antigen specific and the reactivity was restricted to the class I-major histocompatibility complex, as is also shown in Fig. 3 (Figs. 5C and D).

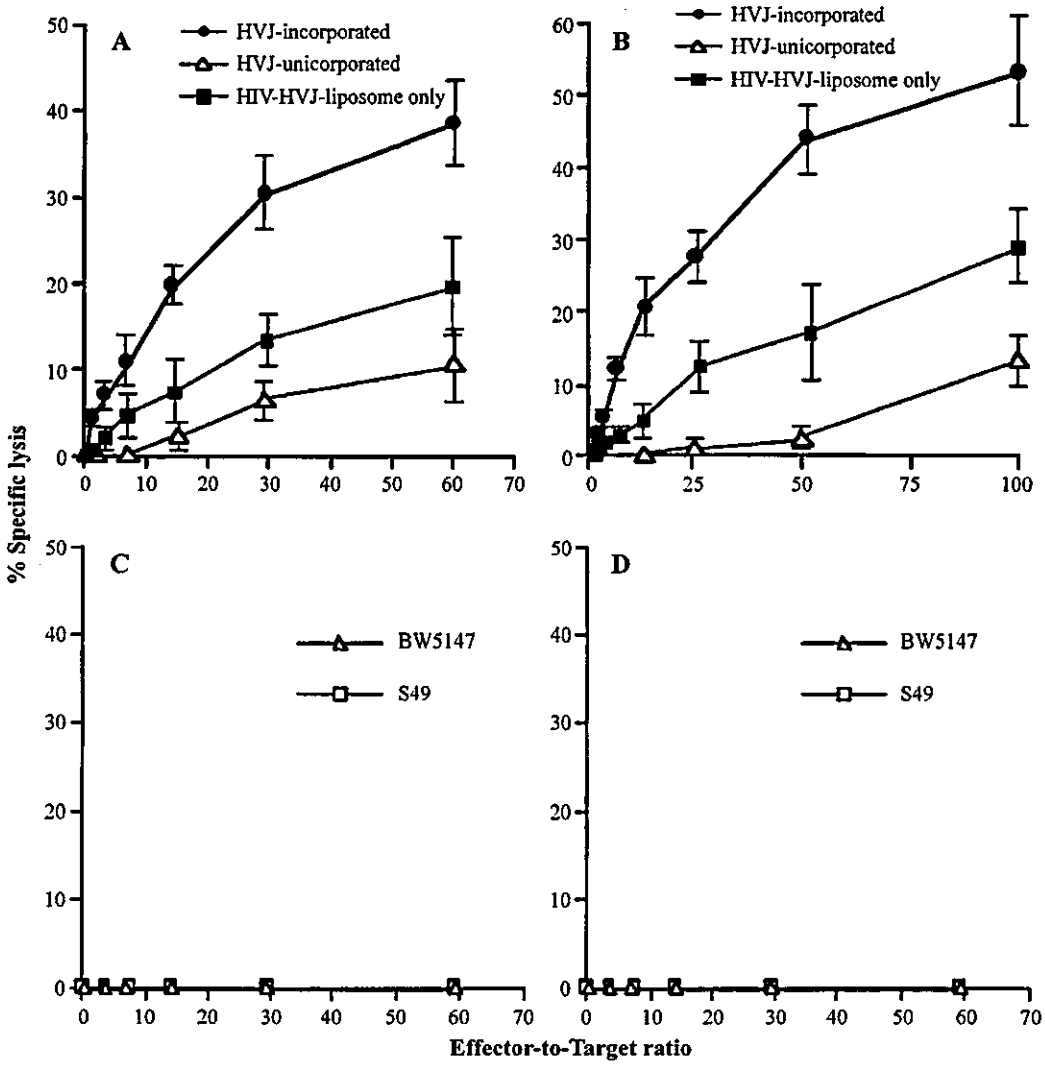

Fig. 5. Effect of the incorporation of the HVJ protein in terms of induction of HIV-1-specific CTL responses in the consecutively vaccinated mice primed with HIV-HBc followed by administration of HVJ-HIV-liposome. (A) Enhancement of HIV-1-specific CTL responses in the consecutively vaccinated mice with HIV-1_{HXB2}-HBc immunization followed by HIV-1_{HXB2}-HBc-liposome. Cytolytic activity was measured against M12.4.5 target cells pulsed or not pulsed with the V3-TIP peptide. The restimulated spleen cells from HIV-HBc-immunized mice followed by HIV-HVJ-liposome or followed by HIV-liposome were incubated with ^{51}Cr-labeled target cells. (●) cytolytic activity of V3-peptide-stimulated spleen cells from animals immunized with HIV-HBc priming followed by boosting with HVJ-incorporated HIV-liposome; (△) cytolytic activity of V3-peptide-stimulated spleen cells from animals immunized with HBc-HIV priming followed by boosting with HVJ-unincorporated HIV-liposome; and (■) cytolytic activity of V3-peptide-stimulated spleen cells from animals immunized with HVJ-incorporated HIV-liposome alone. (B) Similar enhancement of CTL activities was detected by a booster injection of HIV-1_{MN}-HVJ-liposome in animals with a prior immunization with HIV-1_{MN}-HBc injection. The results are expressed as the mean of three different experiments using five mice in each group. (C and D) Cytolysis was restricted to the major histocompatibility complex class I. Cytolysis was measured against BW5147 (△) and S49 (□).

HIV-V3-specific antibody responses were also induced in the HIV-HBc-primed animals boosting of the HIV-HVJ-liposome in the consecutive immunization regimen as well as HIV-HVJ-liposome immunization only. The guinea pigs of the two immunized groups similarly exhibited V3-binding antibody activity at serum dilutions more than 12,800 by HIV_{HXB2} V3 (Fig. 6A) or HIV_{MN} V3 (Fig. 6B) ELISA at 10 weeks after immunization. The serum antibody was purified from the HIV-HBc-immunized guinea pigs followed by the booster injection with HIV-HVJ-liposome or with HIV-liposome without HVJ, or from the animals immunized with HVJ-HIV-liposome only. PBMC-based virus neutralization assay with PBMC-passaged HIV_{LAI}, HIV_{MN} and HIV_{Th22} was used for the analysis (Fig. 6C). Measurements of inhibitory dose of 50% reduction of virus neutralization (ID_{50}) showed that the antibodies type-specifically neutralized the laboratory strain of clade B HIV_{LAI} and HIV_{MN2} with ID_{50} of serum antibodies from the HIV_{HXB2}- or HIV_{MN}-HVJ-liposome-boostered guinea pigs as well as from animals immunized with HIV_{MN}-HVJ-liposome only were approximately 6.5–15.5 μg/ml (Fig. 6C) but not HIV CRF01 AE, HIV_{Th22} (data not shown). However, virus neutralizations were not detected in sera from the HIV-HBc-immunized guinea pigs

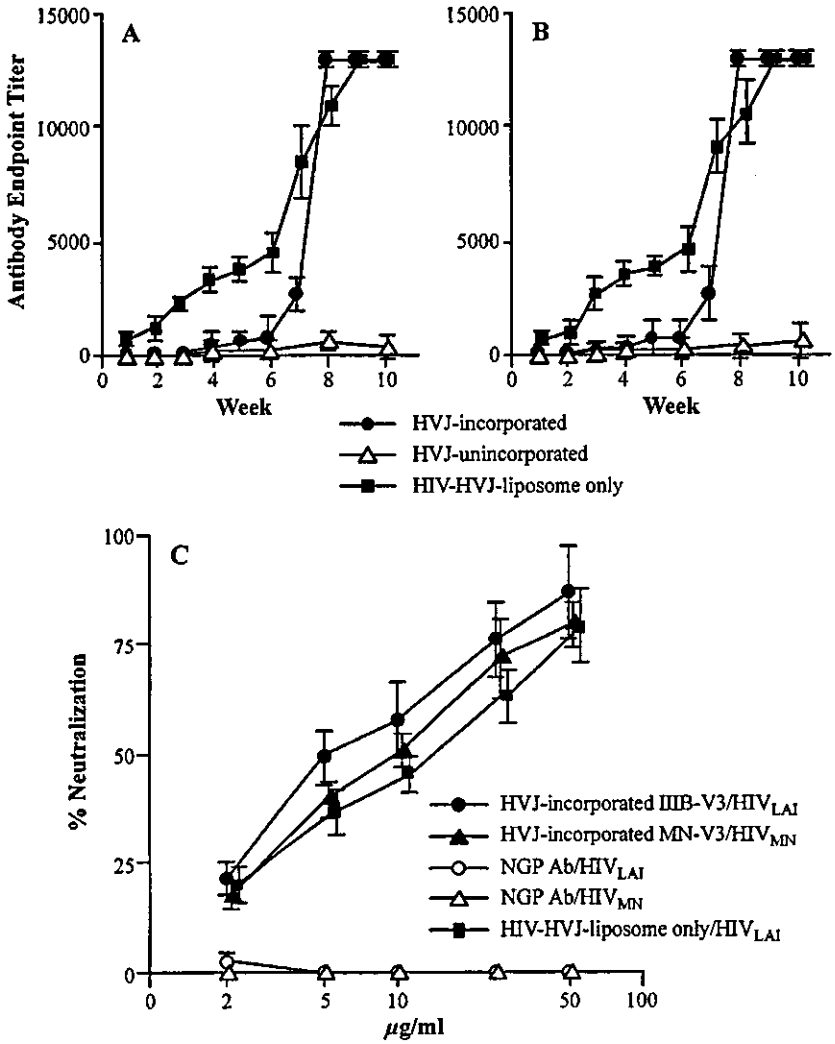

Fig. 6. HIV-1 antibody induction in a consecutive immunization regimen involving HIV-HBc immunization followed by the HIV-HVJ-liposome. HIV-1 antibody titers against HIV_{HXB2} V3 peptide (A) or HIV_{MN} V3 peptide (B) in the immunized animals were measured by ELISA with an endpoint dilution of immune sera. (●), sera from animals immunized with HBc-HIV priming followed by boosting with HVJ-incorporated HIV-liposome; (△) sera from animals immunized with HBc-HIV priming followed by boosting with HVJ-unincorporated HIV-liposome; and (■) sera from animals immunized with HVJ-incorporated HIV-liposome alone. (C) Detection of neutralization activity in the immune sera from the consecutively vaccinated animals. Neutralization activities are expressed as percentage inhibition, compared with control activity, and the mean of four different assays. (●), neutralization activity of serum IgG from animals immunized with HBc-HIV_{IIIB} priming followed by boosting with HVJ-incorporated HIV_{IIIB}-liposome; (▲) neutralization activity of serum IgG from animals immunized with HBc-HIV_{MN} priming followed by boosting with HVJ-incorporated HIV_{MN}-liposome; (○) neutralization activity of normal serum IgG against HIV_{IIIB}; (△) neutralization activity of normal serum IgG against HIV_{MN}; and (■) neutralization activity of serum IgG from animals immunized with HVJ-incorporated HIV-liposome alone.

following booster injections with HVJ-unicorporated HIV-liposome and in the preimmune animals or in naïve animals.

IL-12, IL-18, and IFN-γ productions are induced by stimulation with HVJ protein

We confirmed the HVJ protein-induced enhancement of IL-12, IL-18, and IFN-γ productions of spleen cells from animals immunized with HBc-HIV priming followed by HVJ-HIV-liposome boosting (Fig. 7). The enhanced production was specific to stimulation with HVJ protein for 24 h, but not with nonspecific culture with BSA. The result suggests that IL-18 may synergistically act with IL-12 to enhance IFN-γ production.

Discussion

This report describes a study, when an HVJ protein was incorporated into an HIV-liposome and used as a booster immunization in HIV-HBc-primed animals, the immunized animals demonstrated the induction of a strong HIV-specific $CD4^+$ T-cell response. The animals immunized with a consecutive immunization strategy were characterized. The analysis revealed enhanced cellular and humoral immunities. The findings thus suggest that the incorporation of the HVJ protein into the HIV-liposome significantly affects immunity in animals primed with HIV antigen encapsulated inside an HBc particle. Furthermore, the present results suggest that the HBc particle-based vaccine seems to be a suitable immunogen for an HIV-1 vaccine; this protocol effectively uses a booster immunization of an HIV antigen incorporated in an anionic HVJ-liposome.

In the present study, the HIV-liposome did not induce an HIV-specific proliferative response in HIV-HBc primed animals. However, the HVJ protein induced an immune response when it was incorporated into an HIV-liposome and used as a booster antigen. Moreover, a comparison of the T-cell proliferative responses inducing activity of both anionic-type and cationic-type HIV-HVJ-liposome demonstrated that the anionic liposome was more effective at inducing such activity than the cationic HIV-HVJ-liposome, when both are administered subcutaneously (data not shown). The effectiveness of the HVJ protein incorporation into the HIV-liposome at inducing the T-cell proliferative cell response does not seem to depend solely on the electrical charge, however. Instead, the effect depended on the route of antigen administration. This assumption was made because when the HIV-HVJ-liposome was administered nasally to mice, the HIV-HVJ-liposome was seen to induce antigen-specific CTLs and neutralizing antibody responses [47]. The different effects of HVJ-anionic and -cationic liposomes allow some inferences to be made about the antigen uptake rate into immune-competent cells. We previously developed a highly efficient method of gene transfer involving the entrapment of RNA or DNA using the HVJ protein to enhance the uptake of genes into target cells [48]. In that method, cationic lipids were used for the preparation of the liposome; the transgene expression level thereby significantly improved in cultured cells using this cationic-liposome gene delivery system [39,49]. Cellular uptake to targeted RNA complexed with an HVJ-cationic liposome was measured to be approximately 5 times higher than that of an HVJ-anionic liposome in cultured cell line cells [49]. In this study, we developed a highly efficient method for antigen immunization by delivering the antigen into cells using HVJ-anionic liposomes in experimental

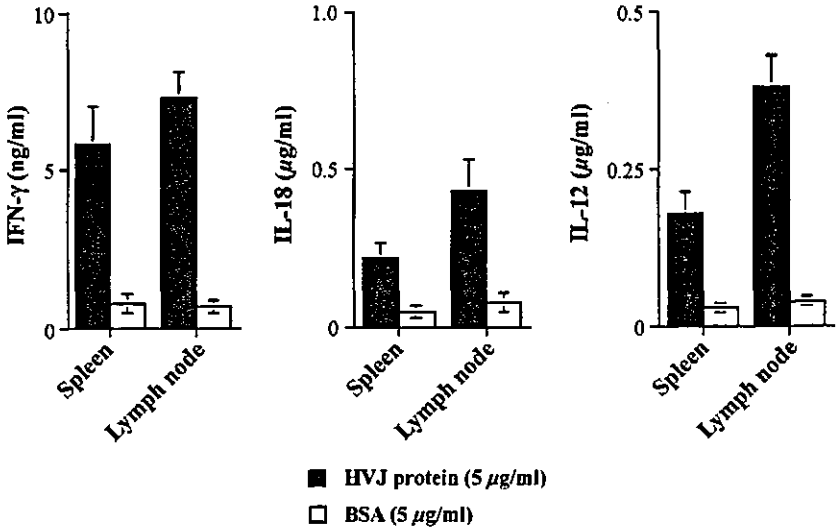

Fig. 7. IFN-γ, IL-18, and IL-12 secretion in HVJ extract-stimulated spleen cells from animals immunized with HBc-HIV priming followed by boosting with HVJ-HIV-liposome. Freshly isolated splenocytes were stimulated with 5.0 μg/ml of HVJ extract or same concentration of BSA for 24 h. Supernatants from separately cultured cells of five different animals were harvested and each cytokine amounts in supernatants were measured by ELISAs. The mean ± SD of three separate experiments is shown.

small animals. According to the present method, the anionic-liposome fused with HVJ was significantly effective at inducing an antigen-specific T-cell proliferative response. In fact, this method proved more effective than the use of antigen-primed animals that had received a booster injection of an HVJ cationic-liposome that was fused with an antigen (data not shown). Collectively, our results indicate that when the induction of antigen-specific T-cell immunity was targeted systemically, the use of an HVJ anionic liposome is suitable, because the antigen may not be localized at the injection site but rather be delivered throughout the body. Furthermore, antigen entrapment was enhanced by the effect of HVJ. However, when the immune induction is targeted locally, the cationic type of HVJ-liposome seems to be more effective as an antigen-delivery system, because the cationic HVJ-liposome effectively fused with the antigen and delivered the target antigen into cells located in a relatively limited region. Our observation also shows that HVJ protein is effective for the induction of an immune response. These findings suggest that enhancement of antigen uptake might be responsible for the induction of effective immune responses.

Concerning the adjuvant effect of the liposomes with HVJ protein, the HVJ protein appears to have the ability to enhance the secretion of immune enhancing cytokines, such as IL-12, IL-18, and IFN-γ, because those cytokines are released form splenocytes by in vitro culture with the HVJ-protein. Our results suggest that IL-18 released from stimulated macrophages may synergistically act with secreted IL-12 to stimulate enhanced production of IFN-γ. Stimulation of spleen cells or T-cell clones with HVJ protein-induced IFNs, TNF-α, and -β in vitro has been reported [50,51]. Thus, stimulation of lymphoid cells by HVJ protein might play a role in the enhanced induction of immunity. Pirhonen et al. [52] reported that the Sendai virus was able to enhance IL-18 level in macrophages, and that the data suggested that indirect immune activation by the effect of IL-18 produced by the stimulation of HVJ protein may also play a role in helper cell induction. This was thought to be because IL-18 can stimulate Th0 cells and promote the differentiation of cells to induce IFN-γ or IL-4 production in the presence or absence of IL-12 [53–55]. This co-stimulation of the immune system by a viral protein or component is commonly seen in the presence of other viruses or bacteria, for example, influenza virus and mycobacterium. The influenza fusion protein was similarly incorporated in fusigenic liposomes and used as a liposome-type adjuvant, namely, Virosome [56]. The advantage of the use of the HVJ protein is that it is known to be a highly fusigenic protein and has even previously been used for cell fusion to produce hybridoma. This method is expected to enhance the uptake of antigens into cells. The results show that repeated inoculations may be acceptable for in vivo use. In conclusion, it seems likely that HVJ protein-incorporated liposomes fused with antigen may enhance antigen uptake to the immunocompetent cells via the HVJ protein. Thus, the HVJ protein may also stimulate helper cells to differentiate and produce cytokines, thus enhancing immune responses.

As described above, the use of the HVJ protein for the preparation of HIV-liposomes allowed us to overcome the difficulty of immune induction induced by immunization of an antigen within the particles. Specifically, we were able to substantially induce a $CD4^+$ T-cell proliferative response. Furthermore, we observed a significant association among the induction of HIV-specific humoral response, and the enhancement of an HIV-specific CTL response due to immunization of HIV-HBc primed animals with the HVJ protein-incorporated HIV-liposome. These marked inductions of immunity are obtained by incorporating the HVJ protein into the anionic HIV-liposome, which were used as a booster antigen in a consecutive immunization regimen. The reason why the HVJ protein was able to induce HIV-specific immunity so effectively in the animal model may be that the consecutive immunization strategy, which employed the HVJ protein, can induce a marked $CD4^+$ T-cell response specific for HIV in the animal. We did not test a group immunized with the HVJ protein mixed with but not incorporated into the HIV-liposome. We speculate, however, that the HVJ protein was incorporated into the HIV-liposomes, and that after the incorporated HVJ peptide and HIV circular V3 peptide were mixed and trapped together on/in the liposome, the mixture was effective. If this is the case, the HVJ protein might be beneficial for forming the protein mixture that will work for the T-cell epitope. This speculation about the mechanism of helper response induction is also supported by the observation that when the HIV-V3 peptide was covalently constructed with an overlapping T-cell epitope peptide, it induced CTL in a non-emulsion adjuvant [57]. When the unlinked but mixed peptides were trapped together, the mixture also worked to some extent in a water-in-oil emulsion adjuvant [58,59]. The significance of the helper T-cell response has been demonstrated in other chronic viral infections [60]. The induction of a $CD4^+$ T-cell response in controlling HIV generation has recently shown that virus-specific T helper lymphocytes are critical for the maintenance of effective immunity in chronic viral infections [11]. The HIV-specific T-cell response is likely to be important in immunotherapeutic interventions [61] and vaccine development [62]. One of the explanations of the role of the $CD4^+$ T cells in CTL induction is that the $CD4^+$ T-cell help was mediated by binding with CD4 ligand on dendritic cells in the expansion of HIV-specific $CD8^+$ memory T-cell responses [63]. In contrast, in the absence of $CD4^+$ T-cell help, adequate CTL activity was not maintained and revealed the persistence of activated virus-specific CTL without effector function [64].

In conclusion, induction of a strong T-cell proliferative response has been obtained in a small animal model by using a consecutive immunization strategy that involved priming with HIV-HBc and boosting with the HIV-HVJ-liposome. Furthermore, it might be demonstrated that an efficacy test for viral challenges may be available.

Acknowledgments

We thank Dr. Yoshiyuki Nagai of the National Institute of Infectious Diseases, Tokyo, for their helpful discussions. This work was supported by the Japan Health Science Foundation, Chuo-ku, Tokyo, Japan and the Ministry of Health, Labor and Welfare, Japan.

References

[1] J. Hansen, T. Schulze, K. Moelling, RNase H activity associated with bacterially expressed reverse transcriptase of human T-cell lymphotropic virus III/lymphadenopathy-associated virus, J. Biol. Chem. 262 (1987) 12393–12396.

[2] X. Wu, H. Liu, H. Xiao, J. Kim, P. Seshaiah, G. Natsoulis, J.D. Boeke, B.H. Hahn, J.C. Kappes, Targeting foreign proteins to human immunodeficiency virus particles via fusion Vpr and Vpx, J. Virol. 69 (1995) 3389–3398.

[3] A. Charbit, P. Martineau, J. Ronco, C. Leclerc, R. Lo-Man, V. Michel, D. O'Callaghan, M. Hofnung, Expression and immunogenicity of the V3 loop from the envelope of human immunodeficiency virus type 1 in an attenuated aroA strain of *Salmonella typhimurium* upon genetic coupling to two *Escherichia coli* carrier proteins, Vaccine 11 (1993) 1221–1228.

[4] C.K. Stover, V.F. de la Cruz, G.P. Bansal, J.F. Young, M.H. Lee, G.F. Hatfull, S.B. Snappe, R.G. Barletta, W.R. Jacobs Jr., B.R. Bloom, New use of BCG for recombinant vaccines, Nature 351 (1991) 456–460.

[5] R.J. Natuk, P.K. Chanda, M.D. Lubeck, A.R. Davis, J. Wilhelm, R. Hjorth, M.S. Wade, B.M. Bhat, S. Mizutani, S. Lee, J. Eichberg, R.C. Gallo, P.P. Hung, M. Robert-Guroff, Adenovirus-human immunodeficiency virus (HIV) envelope recombinant vaccines elicit high-titered HIV-neutralizing antibodies in the dog model, Proc. Natl. Acad. Sci. U. S. A. 89 (1992) 7777–7781.

[6] T. Hanke, R.V. Samuel, T.J. Blanchard, V.C. Neumann, T.M. Allen, J.E. Boyson, S.A. Sharpe, N. Cook, G.L. Smith, D.I. Watkins, M.P. Cranage, A.J. McMichael, Effective induction of simian immunodeficiency virus-specific cytotoxic T lymphocytes in macaques by using a multiepitope gene and DNA prime-modified vaccinia virus Ankara boost vaccination regimen, J. Virol. 73 (1999) 7524–7532.

[7] S.W. Barnett, S. Rajasekar, H. Legg, B. Doe, D.H. Fuller, J.R. Haynes, C.M. Walker, K.S. Steimer, Vaccination with HIV-1 gp120 DNA induces immune responses that are boosted by a recombinant gp120 protein subunit, Vaccine 15 (1997) 869–873.

[8] J.A. Berzofsky, J.D. Ahlers, M.A. Derby, C.D. Pendleton, T. Arichi, I.M. Belyakov, Approaches to improve engineered vaccines for human immunodeficiency virus and other viruses that cause chronic infections, Immunol. Rev. 170 (1999) 151–172.

[9] I.M. Belyakov, L.S. Wyatt, J.D. Ahlers, P. Earl, C.D. Pendleton, B.L. Kelsall, W. Strober, B. Moss, J.A. Berzofsky, Induction of a mucosal cytotoxic T-lymphocyte response by intrarectal immunization with a replication-deficient recombinant vaccinia virus expressing human immunodeficiency virus 89.6 envelope protein, J. Virol. 72 (1998) 8264–8272.

[10] D. Ho, Long-term non-progressor, 10th International Conference on AIDS (Yokohama), vol. I, 1994. p. 50.

[11] E.S. Rosenberg, J.M. Billingsley, A.M. Caliendo, S.L. Boswell, P.E. Sax, S.A. Kalams, B.D. Walker, Vigorous HIV-1-specific $CD4^+$ T cell responses associated with control of viremia, Science 278 (1997) 1447–1450.

[12] J.D. Ahlers, C.D. Pendleton, N. Dunlop, A. Minassian, P.L. Nara, J.A. Berzofsky, Construction of an HIV-1 peptide vaccine containing a multideterminant helper peptide linked to a V3 loop peptide 18 inducing strong neutralizing antibody responses in mice of multiple MHC haplotypes after two immunizations, J. Immunol. 150 (1993) 5647–5665.

[13] T. Fehr, D. Skrastina, P. Pumpens, R.M. Zinkernagel, T cell-independent type I antibody response against B cell epitopes expressed repetitively on recombinant virus particles, Proc. Natl. Acad. Sci. U. S. A. 95 (1998) 9477–9481.

[14] F. Schodel, D.R. Milich, H. Will, Hepatitis B virus nucleocapsid/pre-S2 fusion proteins expressed in attenuated *Salmonella* for oral vaccination, J. Immunol. 145 (1990) 4317–4321.

[15] K. Shiosaki, K. Tanaka, S. Nishimura, H. Mizokami, K. Matsubara, Production of hepatitis B virion-like particles in yeast, Gene 106 (1991) 143–149.

[16] F. Schodel, A.M. Moriarty, D.L. Peterson, J. Zheng, J.L. Hughes, H. Will, D.J. Leturcq, J.S. McGee, D.R. Milich, The position of heterologous epitopes inserted in hepatitis B virus core particles determines their immunogenicity, J. Virol. 66 (1992) 106–114.

[17] K. Townsend, M. Sallberg, J. O'dea, T. Banks, D. Driver, S. Sauter, S.M. Chang, D.J. Jolly, S.J. Mento, D.R. Milich, W.T.L. Lee, Characterization of $CD8^+$ cytotoxic T-lymphocyte responses after genetic immunization with retrovirus vectors expressing different forms of the hepatitis B virus core and e antigens, J. Virol. 71 (1997) 3365–3374.

[18] A. Miyanohara, T. Imamura, M. Araki, K. Sugawara, N. Ohmoto, K. Matsubara, Expression of hepatitis B virus core antigen gene in *Saccharomyces cerevisiae*: synthesis of two polypeptides translated from different initiation codons, J. Virol. 59 (1986) 176–180.

[19] D.R. Milich, A. McLachalan, G.B. Thornton, J.L. Hughes, Antibody production to the nucleocapsid and envelope of the hepatitis B virus primed by a single synthetic T cell site, Nature 329 (1987) 547–549.

[20] B.E. Clarke, S.E. Newton, A.R. Carroll, M.J. Francis, G. Appleyard, A.D. Syred, P.E. Highfield, D.J. Rowlands, F. Brown, Improved immunogenicity of a peptide epitope after fusion to hepatitis B core protein, Nature 330 (1987) 381–384.

[21] A.M. Moriarty, J.S. McGee, B.J. Winslow, D.W. Enman, D.J. Leturcq, G.B. Thornton, J.L. Hughes, D.R. Milich, Expression of HIV gag and env B-cell epitopes on the surface of HBV core particles and analysis of the immune responses generated to those epitopes, in: F. Brown, R.M. Chanock, H.S. Ginsberg, R.A. Lerner (Eds.), Vaccines, vol. 90, Cold Spring Harbor Laboratory, Cold Spring Harbor, NY, 1990, p. 225.

[22] S.J. Stahl, K. Murray, Immunogenicity of peptide fusions to hepatitis B virus core antigen, Proc. Natl. Acad. Sci. U. S. A. 86 (1989) 6283–6287.

[23] G.P. Borisova, I. Berzins, P.M. Pushko, P. Pumpen, E.J. Gren, V.V. Tsibinogin, V. Loseva, V. Ose, R. Ulrich, H. Siakkou, H.A. Rosenthal, Recombinant core particles of hepatitis B virus exposing foreign antigenic determinants on their surface, FEBS Lett. 259 (1989) 121–124.

[24] F. Schodel, T. Weimer, H. Will, D. Milich, Recombinant HBV core particles carrying immunodominant B-cell epitopes of the HBV pre-S2 region, in: F. Brown, R.M. Chanock, H.S. Ginsberg, R.A. Lerner (Eds.), Vaccines, vol. 90, Cold Spring Harbor Laboratory, Cold Spring Harbor, NY, 1990, p. 193.

[25] F. Schodel, D.R. Milich, H. Will, Hybrid hepatitis B virus core/PreS particles expressed in live attenuated Salmonellae for oral immunization, in: F. Brown, R.M. Chanock, H.S. Ginsberg, R.A. Lerner (Eds.), Vaccines, vol. 91, Cold Spring Harbor Laboratory, Cold Spring Harbor, NY, 1991, p. 319.

[26] B.E. Clarke, A.R. Carroll, A.L. Brown, J. Jon, N.R. Parry, E.W. Rud, M.J. Francis, D.J. Rowland, Expression and immunologic analysis of hepatitis-B core fusion particles carrying internal heterologous sequences, in: F. Brown, R.M. Chanock, H.S. Ginsberg, R.A. Lerner (Eds.), Vaccines, vol. 91, Cold Spring Harbor Laboratory, Cold Spring Harbor, NY, 1991, p. 313.

[27] F. Boudet, M. Girard, J. Theze, M. Zouali, Antibodies of HIV-1 positive subjects and experimentally immunized primates and rodents bind to sequence divergent regions of the third variable domain (V3) of gp120, Int. Immunol. 4 (1992) 283–294.

[28] H. Takahashi, J. Cohen, A. Hosmalin, K.B. Cease, R. Houghten, J.L.